Universidade do Minho
Escola de Ciências

Andreia Isabel da Silva Araújo

Thermal and UV stability of PLA nanocomposites

Julho de 2012

Andreia Isabel da Silva Araújo **Thermal and UV stability of PLA nanocomposites**

UMinho | 2012

Universidade do Minho
Escola de Ciências

Andreia Isabel da Silva Araújo

Thermal and UV stability of PLA nanocomposites

Dissertação de Mestrado
Mestrado em Técnicas de Caracterização e Análise Química

Trabalho efetuado sob a orientação da
Professora Doutora Gabriela Botelho
e da
Professora Doutora Ana Vera Machado

Julho de 2012

DECLARAÇÃO

Nome: Andreia Isabel da Silva Araújo

Endereço eletrónico: pg17495@alunos.uminho.pt

Título da tese de mestrado: Thermal and UV stability of PLA nanocomposites

Orientador(es): Professora Doutora Gabriela Botelho e Professora Doutora Ana Vera Machado

Ano de conclusão: 2012

Designação do Mestrado: Mestrado em Técnicas de Caracterização e Análise Química

Universidade do Minho, ___/___/_____

Assinatura: _____

Acknowledgements

This research project could not be possible without the precious help and support of a large number of people around me. Therefore, I would like to express my gratitude to all of them.

First of all, I wish to express my deep gratitude to my supervisors Professor Gabriela Botelho and Professor Ana Vera Machado for giving me the opportunity to carry out this study. I also have to thank their availability, patient guidance, enthusiastic encouragement and sympathy. I would also like to thank Professor Manuela Silva for the help and scientific guidance.

My thanks are also addressed to academic staff, researchers and technicians from Department of Chemistry and Polymer Engineering that helped me along this work. Special thanks to Joana Barbas for all the time she dedicated to me, for her patience, scientific guidance and encouragement.

I am also profoundly grateful to Sérgio, Liliana, Natália, Paulo, Isabel, Beatriz and Ana for the unconditional support, help and care. My grateful thanks are also extended to the new colleagues Daniela, Pedro and Renato for all the encouragement and good moments proportionated, as well as to my other friends and colleagues that were there to make me smile.

Finally, I take this opportunity to sincerely thank my parents for their love, patience and unceasing support since the day I was born.

Thank you all!

Muito obrigada!

Abstract

Poly(lactic acid) (PLA) is a biodegradable aliphatic thermoplastic polyester well known for being a promising alternative to petroleum-based materials as it can be produced from renewable resources at low cost and recyclable to its monomer. Although this polymer has good properties compared to other biodegradable polymers, it presents some limitations, like poor thermal and mechanical resistance and limited gas barrier properties. The incorporation of nanoclays has been used as a way to overcome this problem. Since resistance to UV light is a key factor for polymeric materials used in outdoor applications, it is important to investigate the effect of these nanoparticles.

Thus, the present work aims to investigate the influence of clay type (Cloisite 30B, Cloisite 15A and Dellite 43B) and amount (3 and 5 wt.%) on PLA thermal and UV stability. PLA and PLA nanocomposites prepared by melt mixing were submitted to thermo-oxidative degradation during 120 hours and exposure to UV light in an accelerated chamber for 600 hours. Starting materials and samples removed along the degradation time were characterized by solution viscosimetry, energy-dispersive spectroscopy (EDS), scanning electron microscopy (SEM), X-ray diffraction (XRD), proton nuclear magnetic resonance (^{1}H-NMR), Fourier transform infrared spectroscopy (FTIR), thermogravimetry (TGA) and differential scanning calorimetry (DSC).

The prepared nanocomposites exhibited intercalated structure. However, the presence of nanoclay aggregates was detected in C15A nanocomposites.

Even though after thermo-oxidative degradation all samples exhibited a significant decrease in intrinsic viscosity, it was minor for nanocomposites containing 3 wt.% nanoclays. An increase in the crystallinity degree was also observed for degraded nanocomposites.

UV ageing results showed that the presence of nanoclays in PLA matrix induces polymer photo-degradation, as higher decrease of intrinsic viscosity and changes in chemical structure were observed. FTIR spectra of degraded C30B nanocomposites indicate that anhydride groups are formed during photo-degradation.

PLA nanocomposites prepared in the present work exhibited higher thermal stability and lower photo stability than PLA.

Resumo

O ácido poli-láctico (PLA) é um poliéster alifático biodegradável conhecido por ser um promissor substituto de materiais derivados de petróleo, uma vez que pode ser produzido a partir de recursos renováveis de baixo custo e reciclável até à obtenção do monómero. Embora este polímero apresente boas propriedades, quando comparado com outros polímeros biodegradáveis, também apresenta algumas limitações como baixa resistência térmica e mecânica e propriedades de barreira limitadas. A incorporação de nanoargilas em PLA tem sido utilizada como forma de ultrapassar estas limitações. No entanto, como a resistência à radiação é um fator chave nos materiais poliméricos quando utilizados em aplicações exteriores, é necessário investigar o efeito destas nanopartículas.

Assim, o presente trabalho tem como objetivo investigar a influência do tipo de nanoargila (Cloisite 30B, Cloisite 15A e Dellite 43B) e quantidade (3 e 5 %) na estabilidade térmica e UV do PLA. Os nanocompósitos de PLA foram submetidos a 120 horas de degradação termo-oxidativa e a 600 horas de exposição à radiação UV numa câmara de degradação acelerada. Os materiais iniciais e amostras retiradas ao longo do tempo foram caracterizados através de viscosidade de soluções, espetroscopia de dispersão de energia de raios-X (EDS), microscopia eletrónica de varrimento (SEM), difração de raios-X (XRD), espetroscopia de infravermelho com transformadas de Fourier (FTIR), termogravimetria (TGA) e calorimetria diferencial de varrimento (DSC).

A caracterização das amostras iniciais mostrou que se obtiveram nanocompósitos com estrutura intercalada, mas com a nanoargila C15A verificou-se a presença de agregados.

Após degradação termo-oxidativa, todas as amostras exibiram uma diminuição da viscosidade intrínseca, que foi menos acentuada no caso dos nanocompósitos com adição de 3% de nanoargila. Verificou-se ainda um aumento da cristalinidade nas amostras degradadas.

Nas amostras expostas à radiação UV constatou-se que a presença de nanoargilas induziu a foto-degradação do PLA, uma vez que ocorreu maior diminuição de viscosidade intrínseca e maiores alterações na estrutura química. Os espectros de FTIR dos nanocompósitos com C30B evidenciaram a formação de grupos anidrido durante a degradação.

Os nanocompósitos de PLA preparados neste trabalho apresentam maior estabilidade térmica e menor estabilidade à radiação UV que o PLA.

Table of contents

List of abbreviations and symbols

ASTM	American Society for Testing of Materials
C15A	Cloisite 15A
C30B	Cloisite 30B
d_{001}	Diffraction plane 001
D43B	Dellite 43B
DSC	Differential Scanning Calorimetry
EDS	Energy Dispersive X-ray Spectroscopy
FTIR	Fourier Transformed Infrared Spectroscopy
ISO	International Standards Organization
MMT	Montmorillonite
NMR	Nuclear Magnetic Resonance Spectroscopy
PBAT	Poly(butylene adipate-co-terephthalate)
PBSA	Poly(butylene succinate-co-adipate)
PCL	Polycaprolactone
PDLLA	Poly(D-L-lactic acid)
PE	Polyethylene
PEA	Polyesteramide
PET	Poly(ethylene terephthalate)
PHA	Poly(hydroxy-alkanoate)
PHB	Poly(hydroxybutyrate)
PHBV	Poly(hydroxybutyrate-co-hydroxyvalerate)
PLA	Poly(lactic acid)
PLLA	Poly(L-lactic acid)
PP	Polypropylene
PS	Polystyrene
PVC	Poly(vinyl chloride)
SEM	Scanning Electron Microscopy
TEM	Transmission Electron Microscopy
T_g	Glass Transition Temperature
TGA	Thermogravimetry
T_m	Melting Temperature
UV/vis	Ultra Violet/Visible Spectroscopy
WAXS	Wide Angle X-ray Scattering

XRD	X-ray Diffraction
γ	Out-of-plane Bending Vibration
γ_{as}	Asymmetric out-of-plane Bending Vibration
δ	Chemical Shift
δ_{as}	Asymmetric Bending Vibration
δ_{s}	Symmetric Bending Vibration
ΔH°_{m}	Melting enthalpy for polymer 100% crystalline
ΔH_{m}	Experimental Melting Enthalpy
η	Intrinsic Viscosity
η_{r}	Relative Viscosity
ν	Stretching Vibration
ν_{as}	Asymmetric Stretching Vibration
ν_{s}	Symmetric Stretching Vibration
χ	Crystallinity degree

List of Figures

List of Tables

Chapter 1

Context, aim and thesis outline

"The scientist is not a person who gives the right answers; he's one who asks the right questions."

— Claude Lévi-Strauss

This thesis begins with a brief introduction to polymers and nanocomposites. The purpose of this chapter is to describe the context of the work, the overall objectives of the study and the structure of the thesis.

1.1. Context

A polymer is a substance whose molecules form long chains, usually several thousands atoms long. The name polymer is derived from the Greek *poly* for many and *meros* for parts [1], meaning "many parts". Polymers are characterized, and differ from one another, through the chemical and physical nature of the *repeating units*, the monomers, in the chain [2-4]. In order to form polymers, monomers either have reactive functional groups or double (or triple) bonds whose reaction provides the necessary linkages between the repeating units [5].

Polymeric materials usually have high strength, exhibit rubber elasticity, and have high viscosity as melts and solutions. In fact, exploitation of many of these unique properties has made polymers extremely useful to mankind [5-7]. From the earliest times, man has exploited naturally occurring polymers [4]. Although many people probably do not realise it, everyone is familiar with polymers [8, 9]. In fact it is quite inconceivable to most people that we could ever have existed without them. Consider transport, energy production and transmission, agriculture, the building industry, clothing, consumer goods, packaging, food and the health and pharmaceutical industries; all these activities rely heavily on polymeric materials [10, 11]. The polymeric products can take on many forms such as viscous liquids, fibers, films, mouldings, composites powders and granules. The characterization of these materials has been pursued with great vigour in recent years [12].

From the beginning, polymer science has involved physicists, chemists, engineers, materials scientists and design engineers. The multidisciplinary nature of polymer science from its earliest days is a feature that is not often exhibited by other fields of natural science until certain "maturity" has been reached [13].

In recent years the nanoscale, and the associated excitement surrounding nano-science and technology, has afforded unique opportunities to create revolutionary material combinations [14]. The field of nanotechnology is one of the most popular areas for current research and development in basically all technical disciplines [15]. Nanotechnology, by definition, is the creation and subsequent utilization of structures with at least one dimension in the nanometer length scale (i.e. less than 100 nm) that

creates novel properties and phenomena not displayed by either isolated molecules or bulk materials [16, 17].

Nanocomposite technology is a newly developed field, in which nanofillers are added to a polymer to reinforce and provide different characteristics [17]. Nanocomposites are multiphase solid materials in which one of the phases has one, two or three dimension smaller than 100 nm [18, 19].

Today, industrial applications of nanomaterials can be found in a wide variety of fields: applications in electronics and in health care; synthetic textiles incorporating nanopowders that endow the fabrics with antibacterial properties, flame retardant, non-wetting, or self-cleaning properties; thick and thin coatings; buildings and construction; automotive and aerospace components, in environmental remediation and energy storage technologies [11, 14, 15].

The interest in nanotechnology has continuously increased in recent years and it includes all kinds of polymers [20] but specially biodegradable polymers because of increasing environmental concerns about petrochemical based polymers and waste pollution [21-23].

1.2. Aim of the thesis

Researchers work everyday to find out new nanocomposites with improved properties. Degradation is an important process with great influence on polymers behaviour and hinders specific applications. However, degradation may be desirable if post life biodegradation is looked for.

The objective of this thesis is to evaluate the influence of different nanoclays addition (Cloisite 30B, Cloisite 15A and Dellite 43B) on the thermal and UV stability of poly(lactic acid) (PLA). To achieve this aim, PLA nanocomposites with different nanoclays amounts were prepared and then subjected to thermo and photo-oxidative degradation. Samples were characterized before and along degradation time by several techniques.

1.3. Thesis outline

This thesis is divided in six main chapters and each one contains section and subsections.

This chapter (**Chapter 1**) presents a brief context of the research work about polymers and nanocomposites, the aim of the work and the thesis outline.

The state of the art is described in **Chapter 2**, providing information on the PLA and PLA nanocomposites with nanoclays.

Chapter 3 is dedicated to the description of the experimental work, including materials, equipment and methodologies used in the preparation, characterization and degradation of the nanocomposites.

The obtained experimental results and discussion are presented in **Chapter 4.**

Chapter 5 summarizes the most important conclusions of this thesis.

Finally, future perspectives are presented in **Chapter 6** as well as some suggestions for further research.

Chapter 2

Stat of art

“What we know is a drop, what we don't know is an ocean.”

— Isaac Newton

This chapter provides a general overview of the relevant state of the art for this thesis. First in this chapter is defined the importance of the use of biodegradable polymers and their classification according to their origin. Furthermore, the properties and characteristics of PLA are described, as well as its degradation types and applications. In the latter part of the chapter the characteristics of the clays used in this work and the importance of their addiction into polymer matrix will be presented, as well as the preparation and characterization of nanocomposites.

2.1 Environmental concern

The industrial revolution brought unimaginable benefits to humanity in terms of optimised material and energetic products and processes, together with increased living standards for most societies, but has also compromised the fragile environmental equilibrium of the Earth [24].

Nowadays, the plastic industry occupies a predominant and growing place in our everyday life [25] and an extensive variety of petroleum-based synthetic polymers, like polyethylene (PE), polypropylene (PP), polystyrene (PS), poly(ethylene terephthalate) (PET) and poly(vinyl chloride) (PVC), are produced worldwide to an extent of approximately 140 million tons per year [26, 27]. Most of these materials are made for one-use applications or have a relatively short lifetime, being rapidly discarded into the environment once they are consumed and their elimination and reintegration into the carbon cycle can require hundreds or even thousands of years [28, 29].

The three main strategies available for the management of plastic waste are incineration, landfill and recycling [27].

Incineration has the advantage that the plastics have high calorific value and incineration plants can be modified to recover energy from polymers combustion. However, this method produces large amounts of carbon dioxide and often produces toxic gases, which contribute to global warming and global pollution [27, 30].

The storage of wastes at landfill sites is another possibility, but due to the fast development of society these kinds of places are quite limited. On the other hand, burial of plastic wastes in landfill is a time bomb, with today's problems being shifted into the shoulders of future generations [30].

Recycling somehow solves the problem turning wastes back into naphtha, monomers or other oil derivatives [27, 31]. However it requires a considerable higher amount of labour and energy: removal of plastics wastes, separation according to the plastics type, washing, drying, grinding and, only then, reprocessing to final product,

making the produced material more expensive and less lacking quality, when compared to the primary manufactured ones. Plastic identification codes are one aid to separation that has been introduced, and mechanical sorting based on the specific gravity of the different polymers is well developed [27]. Legislation also prevents the use of recycled polymers in direct food contact packaging and plastics with high technical specification [27].

With this background, academic and industrial researchers look for the development of novel materials labelled as "*environmentally-friendly*": materials produced from alternative resources, with lower energy consumption, biodegradable and non-toxic to the environment [25, 32, 33]. Biodegradable polymers play a key-role in solving this problem and during the last 2 decades an exponential rising number of patents and articles about these materials have been published [24].

Some initiatives have been undertaken to facilitate the introduction of biodegradable polymers into society like the banishment of grocery plastic bags responsible for so-called "*white-pollution*" around the world. Globally, bioplastics make up nearly 300,000 metric tons of the plastic market but this represents less than 1% of synthetic plastics produced each year. Nevertheless, the bioplastic market is growing by 20-30% each year [26].

2.2 Biodegradable polymers

Several definitions of biopolymers, biodegradable polymers, biocomposites and other bio-words have been suggested during de last years [24].

The proposed definition for biopolymers involves materials consisting of units that are entirely or in part derived from biomass (e.g. materials with biological origin). It is necessary to distinguish natural polymers amongst biopolymers; natural polymers are defined as polymeric materials obtained from nature, e.g. cellulose, starch, proteins. In this case, all natural polymers can be considered as biopolymers, but not all biopolymers are natural polymers [24].

The American Society for Testing of Materials (ASTM) and the International Standards Organization (ISO) define degradable plastics as those that undergo a significant change in chemical structure under specific environmental conditions. These changes result in a loss of physical and mechanical properties, measured by standard methods [34].

According to ASTM standard D-5488-94d, biodegradable means that the material can undergo decomposition into carbon dioxide, methane, water, inorganic compounds

or biomass, in which the predominant mechanism is the enzymatic action of micro-organisms that can be measured by standard tests, over a specific period of time, reflecting available disposal conditions [35].

Biodegradable polymers are then defined as those that undergo microbially induced chain scission leading to the mineralization. Specific conditions in term of pH, humidity, oxygenation and the presence of some metals are required to ensure the biodegradation of some polymers [30].

A vast number of biodegradable polymers or their monomers are chemically synthesized or biosynthesized during the growth cycles of all organisms. Figure 2.1 proposes a classification with four different categories, depending on the polymers origin [32]:

(i) polymers from biomass such as the agro-polymers from agro-resources;

(ii) polymers obtained by microbial production;

(iii) polymers chemically synthesized using monomers obtained from agro-resources;

(iv) polymers whose monomers and polymers are both obtained by chemical synthesis from fossil resources.

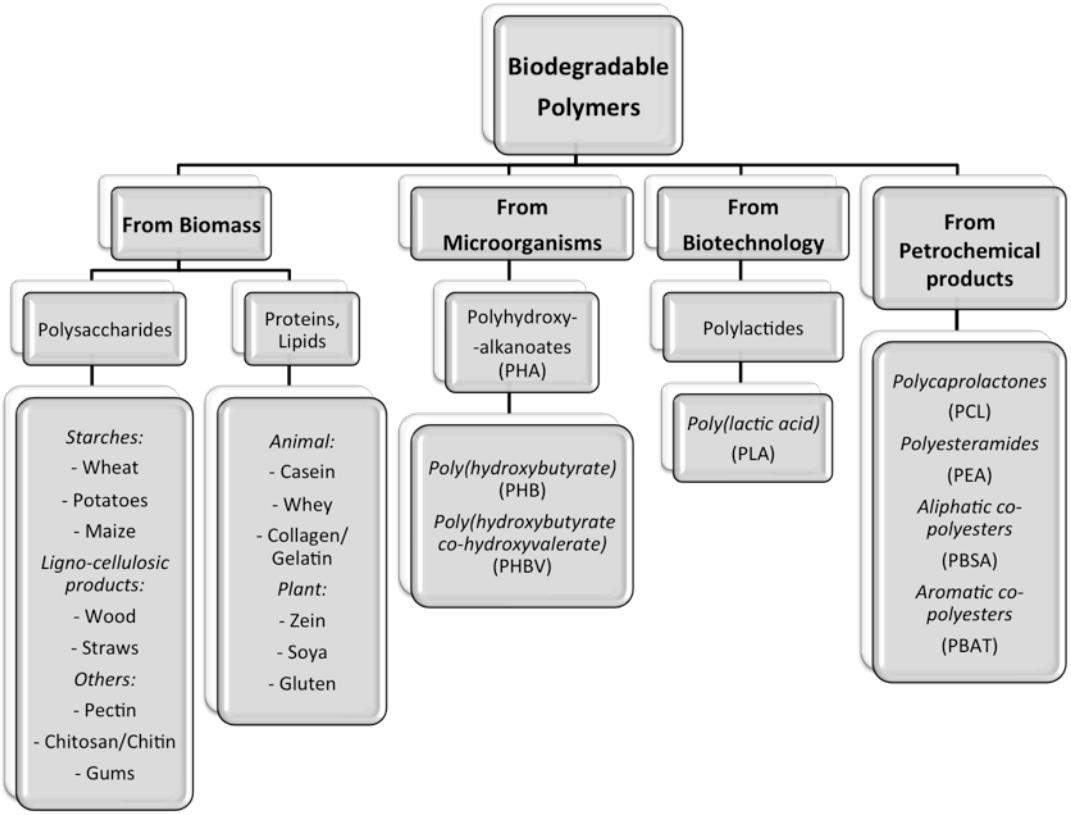

Figure 2.1 - Classification of biodegradable polymers [32].

These different biodegradable polymers can also be sorted into two main families, the agro-polymers (category i) and the biodegradable polyesters (categories ii - iv), also called biopolyesters [32].

2.3 Poly(lactic acid) (PLA)

Among biodegradable polyesters, the family of polylactides (PLA) has recently received a great deal of investigations [36]. PLA is a linear aliphatic thermoplastic polyester, consisting of repeating unities of lactic acid. Lactic acid (2-hydroxypropionic acid), a naturally occurring organic acid, is an optically active molecule that exists in both L and D stereoforms [26, 37].

Renewable resources, such as sugar and corn, can be processed to produce D-glucose, which is then fermented to produce lactic acid (Figure 2.2) [36] by optimized strains of *Lactobacillus* [38]. The biotechnological production of lactic acid offers several advantages compared to chemical synthesis like low cost of substrates, low production temperature, low energy consumption and high product specificity, as it produces desired optically pure L or D lactic acid. Using an appropriated catalyst and heat, there are two major routes to produce PLA: direct condensation polymerization of lactic acid or conversion of lactic acid to the cyclic lactic dimmer and induction by ring opening polymerization through the lactide intermediate, as it can be seen in Figure 2.3 [26, 36, 39, 40].

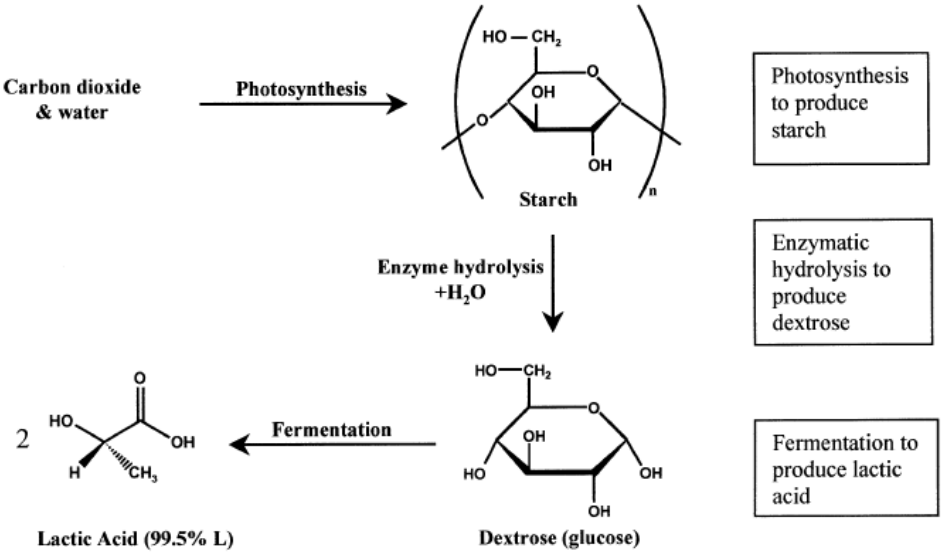

Figure 2.2 – Production of lactic acid by fermentation [39].

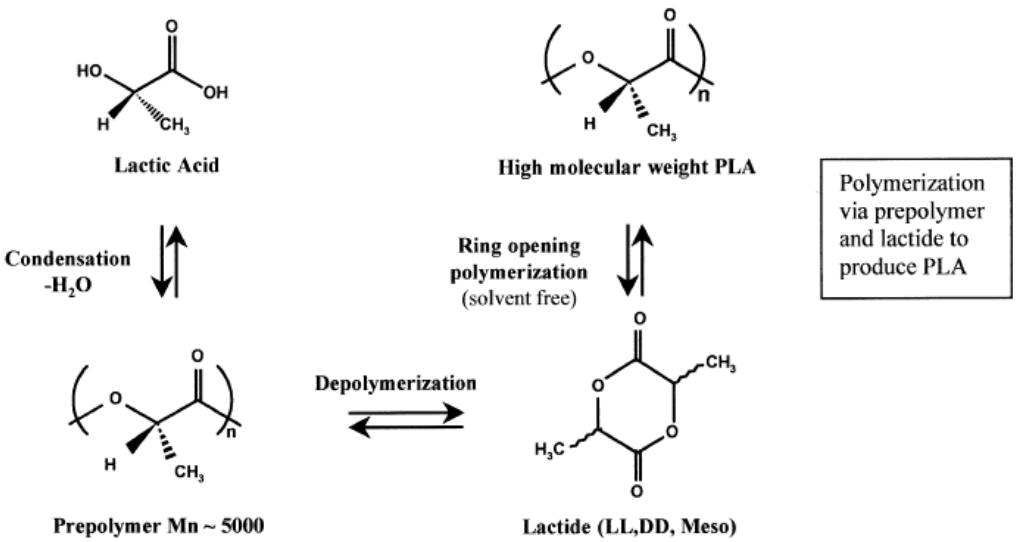

Figure 2.3 - Production of PLA by ring opening polymerization of lactide [39].

Poly(L-lactide) (PLLA) and poly(D-lactide) (PDLA) are prepared by incorporating 100% L or D unities, respectively, and poly(D-L-lactic acid) (PDLLA) by a racemic mixture of L and D isomers (Figure 2.4) [37]. Properties of PLA depend on the processing temperature, annealing time and molecular weight, as well as the amount of D enantiomers that is known to affect particularly de degree of crystallinity [26, 30, 36].

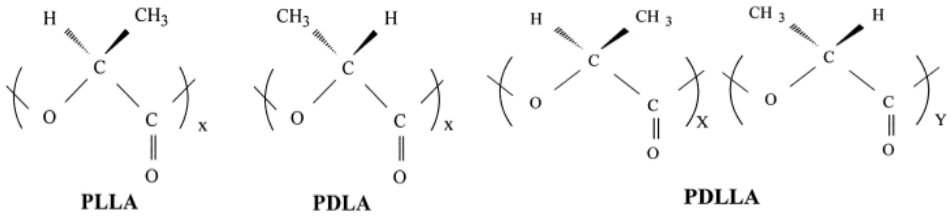

Figure 2.4 - Structure of the different polylactides [41].

PLLA has a crystallinity of around 37%, a glass transition temperature between 50–80 °C and a melting temperature between 173–178 °C. Because of the stereo regular chain microstructure, optically pure polylactides, poly (L-lactide) (PLLA) and poly (D-lactide) (PDLA), are semi crystalline. In general, polylactides are soluble in dioxane, acetonitrile, chloroform, methylene chloride, 1,1,2-trichloroethane and dichloroacetic acid. Ethyl benzene, toluene, acetone and tetrahydrofuran only partly dissolve polylactides when cold, though they are readily soluble in these solvents when heated to boiling temperatures. PLA is a clear, colourless thermoplastic when quenched from the melt and is similar in many aspects to polystyrene [26, 42, 43].

2.4 Degradation

The polymer selected for a certain application depends on its chemical structure and degradation suitable to occur. Two kings of processes may be distinguished, physical and chemical, and both are strongly linked [44]. In nature, polymer degradation is induced by thermal activation, hydrolysis, biological activity (i.e., enzymes), oxidation, photolysis, or radiolysis. Because of the coexistence of biotic and abiotic processes, the entire mechanism of polymer degradation could be, in many cases, referred as environmental degradation. A variety of chemical, physical and biological processes and thus different degradation mechanisms can be involved with the degradation of a polymer [26]. In practice, any change of the polymer properties relative to the initial or desirable properties is called "degradation". In this sense, degradation is a generic term for several reactions that can occur in a polymer and ultimately lead to structural changes, deterioration of the quality of the polymeric materials (i.e. worsening of its mechanical, electrical or esthetic properties) and finally to the loosening of its functionality. This degradation maybe either undesirable when it affects the period of use, or desirable if post life biodegradation is looked for [44]. From an ecological and environmental point of view, development of photodegradable and biodegradable polymers is fundamental [44].

2.4.1. Thermal Degradation

Thermal degradation of polymers can be defined as "molecular deterioration as a result of overheating". At high temperatures the components of the long chain backbone of the polymer can start to separate (molecular scission) and react with another molecules to change the polymer properties [45]. The thermal degradation can be classified into two categories: the thermal degradation in the absence of oxygen (thermal decomposition) and the thermal degradation in the presence of oxygen (thermal oxidation) [46].

Several factors can affect the thermal stability of polymers, like the presence of additives, molecular weight of sample, moisture, hydrolyzed monomers and oligomers, chain end structure, and residual metals. Compounds of metals, such as Sn, Zn, Al, Fe, Zr, Ti, Ca and Mg affect the degradation behavior of PLA to bring down the thermal degradation temperature [47-51].

Research work on the mechanism of thermal degradation of PLA can be summarized as follows: (I) Intra- and intermolecular ester exchange, which leads to the appearance of lactide and cyclic oligomers, is the dominant reaction pathway. (2) The cis-elimination for polyesters, which results in small amount (<5%) of acrylic acid and

acrylic oligomers, is occurring, but is not at all a dominant reaction even at high pyrolysis temperatures. (3) Unzipping depolymerization (backbiting degradation) is also observed. The lower the molecular weight, the more concentrated are the terminal hydroxyl groups, which accelerate the unzipping depolymerization and the intermolecular ester exchange. (4) Pyrolytic elimination of poly(lactic acid) results in species containing conjugated double bonds due to the carbonyl group [42].

McNeill and Leiper [52] proposed that thermal degradation of PLA is a non-radical, "backbiting" ester interchange reaction involving the -OH chain ends. Depending on the point in the backbone at which the reaction occurs, the product can be a lactide molecule, an oligomeric ring, or acetaldehyde plus carbon monoxide (Figure 2.5).

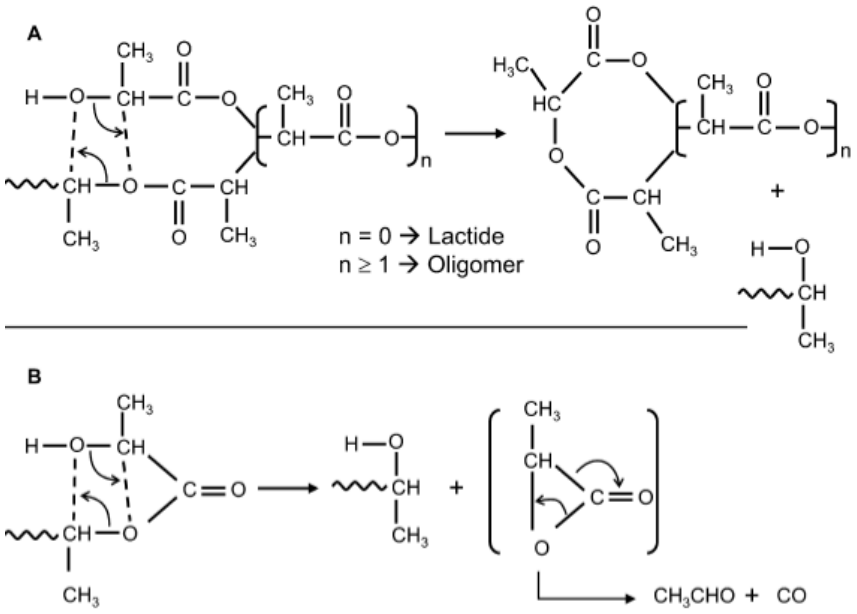

Figure 2.5 – Thermal degradation mechanism of PLA [42].

2.4.2. Photo-degradation

Photo-degradation is the process of decomposition of the materials by the action of light, which is considered as one of the primary sources of damage exerted upon polymeric substrates at ambient conditions. Normally the near-UV radiations (290-400 nm) in the sunlight determine the lifetime of polymeric materials in outdoor applications [53]. However, the polymer materials are irradiated by UV not only at outdoor by exposure to sun light, but also indoor by exposure to fluorescent light [46, 54]. Photo-degradation changes the physical and optical properties of polymers. The most damaging effects are the visual effect (yellowing), the loss of mechanical

properties of the polymers, the changes in molecular weight and the molecular weight distribution [53].

Norrish type I and type II are typical photo-degradation processes. PLA photo-degradation through a Norrish II mechanism is schematically shown in Figure 2.6 and occur structural changes occur as chain cleavage formation of C=O double bonds and hydroperoxyde O-H at newly formed chain terminals [44, 55-58].

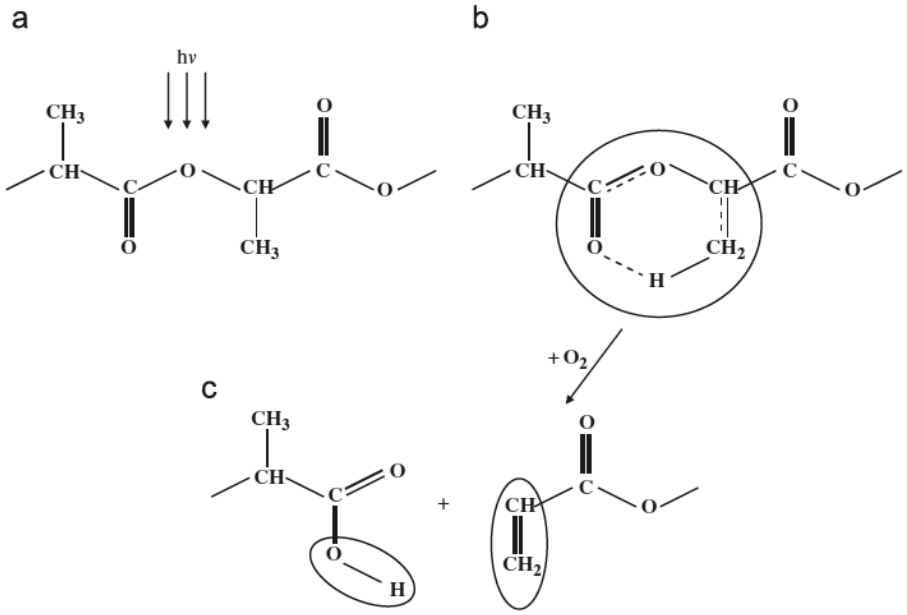

Figure 2.6 - Norrish II mechanism for PLA photo-degradation: (a) PLA chain under UV irradiation, (b) photophysical excitation, and (c) oxidation and scission reactions in PLA chains [44].

As in thermal degradation, photo-degradation can be classified into two categories: the photo-degradation in the absence of oxygen (photo-decomposition) and the photo-degradation in the presence of oxygen (photo-oxidation). Comparison studies show that degradation products from both mechanisms were similar; however, the amounts of the products generated under air condition were higher because of the influence of oxidation [46].

There are two methods to evaluate the photo-degradation of polymers:

Natural weathering method - Outdoor exposure can be performed according to ASTM D-1435-05 on samples mounted on testing racks, oriented under standard conditions to expose the material to the full radiation spectrum besides the temperature and humidity of the location. In order to observe the aging of the material, it is characterized with respect to mechanical properties (elongation at break, tensile properties or impact strength) and visible characteristics, such as crack formation,

chalking, and changes in color. The alterations in the polymeric materials on exposure can be characterized with FTIR spectroscopy and ultra violet/visible (UV/vis) spectroscopy. The disadvantage of this method is that most experiments tale long time periods [53].

Artificial weathering method/laboratory test - Laboratory testing involves the use of environmental chambers and artificial light sources to approximately replicate outdoor conditions, with a great reduced on the testing time and under highly controlled conditions. Several equipments have been used in accelerated aging tests (Atlas Weatherometer Ci 3000, Atlas Uvcon, Atlas XR 260 weatherometer, Xenotest Type 450, Suntester, QUV and Sepap) to predict the polymer lifetime under service conditions [59, 60]. Laboratory testing can quickly assess the relative stability of plastics [53]. However, the correlation between accelerated and natural weathering is not trivial and depends of many agents: accelerated weathering devices, geographical localization in natural experiments, temperature, amount of sunshine hours, mechanical stresses, biological attack, and environmental contaminants [59, 61]. In this work it was used a Xenotest chamber as filtered Xenon lamp present an UV spectrum comparable to UV spectrum of the sun and this pattern of light sources, at low temperature, is expected to be representative of outdoor aging [59].

2.4.3. Chemical degradation

The polymeric materials used in outdoor applications face some hurdles concerning the chemical degradation, as the products for outdoor use are exposed to rain, sunlight, temperature, and environmental bacteria. Hydrolytic degradation occurs not only under water but also under atmospheric condition. The moisture of the air has also a great influence on the polymers hydrolysis [46].

The hydrolytic degradation of PLA has been reported to take place mainly in the bulk of the material rather than on the surface and has been assumed as an autocatalytic hydrolysis, which occurs homogeneously along sample cross-section. The formation of PLA oligomers, which follows the chain scission, increases the carboxylic acid end groups concentration in the degradation medium, making the hydrolytic degradation of PLA a self-catalyzed and self-maintaining process [62]. In parallel, the physical structure of PLA has been found to affect the hydrolytic degradation mechanism, as the hydrolytic chain cleavage proceeds preferentially in the amorphous regions, leading therefore to an increase of the polymer crystallinity [63]. The rate of degradation reaction is also affected by the shape of the samples and by the conditions under which the hydrolysis is

performed, including pH and temperature. High temperatures accelerate the hydrolytic degradation process [64].

2.4.4. Biological degradation

Biodegradation is a biochemical transformation of compounds in mineralization by microorganisms. Mineralization of organic compounds yields carbon dioxide and water under aerobic conditions, and methane and carbon dioxide under anaerobic conditions. Abiotic hydrolysis, photo-oxidation and physical disintegration may enhance biodegradation of polymers by increasing their surface area for microbial colonization or by reducing molecular weight. Biodegradability is also defined as the propensity of a material to get breakdown into its constituent molecules by natural processes (often microbial digestion). The metabolites released by degradation are also expected to be non-toxic to the environment and redistributed through the carbon, nitrogen and sulfur cycles. Biological degradation is chemical in nature but the source of the attacking chemicals is from microorganisms. These chemicals are of catalytic nature e.g. enzymes. Biodegradation of polymers occurs through four different mechanisms: solubilization, charge formation followed by dissolution, hydrolysis and enzyme-catalyzed degradation [53, 65].

Petrochemical-based plastic materials are not easily degraded in the environment because of their hydrophobic character, additionally the three-dimensional structure interferes with the formation of a microbial bio-film, leading to a reduced biodegradation extent [53].

2.5 Applications

PLA presents a wide range of applications and this could be divided into three main categories: biomedical, agricultural and industrial applications.

Biomedical applications of biodegradable and biocompatible polymers generate an enormous amount of research and interest [27]. PLA is one of the most frequently used polyester in biomedical applications due to it many favourable characteristics, such as high strength and biocompatibility [38, 64]. As PLA is derived from monomers that are natural metabolites of the body, the degradation of these materials yields the corresponding hydroxyl acid, making him safe for in vivo use [26]. PLA can be used in repair and regeneration of healing tissues (suture, wound dressings, surgical implants, prosthetic devices) [26, 27, 37, 64] and is one of the best defined biomaterials with regard to design and performance in drug release in a controlled manner [26].

In agricultural applications PLA can be used for controlled release of fertilizers and pesticides [27]. Greenhouse studies confirmed that PLA increased soybean leaf area, pod number, bean number and bean and plant dry weight, suggesting that use of PLA as an encapsulation matrix for herbicides could provide reduced environmental impact and improved weed control and at the same time increasing yield of soybeans through release of plant growth stimulants in the form of oligomeric or monomeric lactic acid [26].

Polylactides fulfil many requirements of packaging thermoplastics and are being developed as commodity resins for general packaging applications like loose-fill packaging, compost bags, food packaging and disposable tableware [26, 37]. Dannon and McDonald's (Germany) pioneered the use of PLA as a packaging material in yogurt cups and cutlery. NatureWorks LLC polymers have been used for a range of packaging applications such as high-value films, rigid thermoformed containers, and coated papers. BASF's Ecovio®, which is a derivative of petrochemical-based biodegradable Ecoflex® and contains 45 wt.% PLA, has been used to make carrier bags, compostable can liners, mulch film, and food wrapping [38, 66].

In the form of fibers and non-woven textiles, PLA also has many potential uses as upholstery, disposable garments, awnings, feminine hygiene products and nappies [26].

Whatever the application, there is often a natural concern regarding the durability of polymeric materials partly because of their useful lifetime, maintenance and replacement. The deterioration of these materials depends on the duration and the extent of interaction with the environment [67].

2.6. Nanocomposites

2.6.1. Importance of clays addition

The main limitations of PLA towards wider industrial application are poor thermal resistance and limited gas barrier properties, which prevent its complete access to industrial sectors such as food packaging [21, 26, 68]. Some of the other properties of PLA, such as melt viscosity, impact resistance, heat distortion temperature, are also not enough for various end-use applications [29, 69] and different nanomaterials have been incorporated into PLA matrix to overcome this problem [21]. Nanoreinforcements of biodegradable polymers results in very promising materials since they show improved properties with preservation of the material biodegradability and without eco-toxicity [32, 70].

Nanomaterials are classified into three categories: nanoparticles, nanotubes and nanolayers [70]. The addiction of clays (nanolayers) is one of the most cost-effective methods to improve the physical properties of PLA [71].

2.6.2. Clays

Clays are ubiquitous minerals, which constitute a large part of the sediments, rocks and soils. Clay minerals belong to the family of phyllosilicates (or layered silicate). The fundamental building units of phyllosilicates (and then of clay minerals) are tetrahedral and octahedral sheets [72, 73].

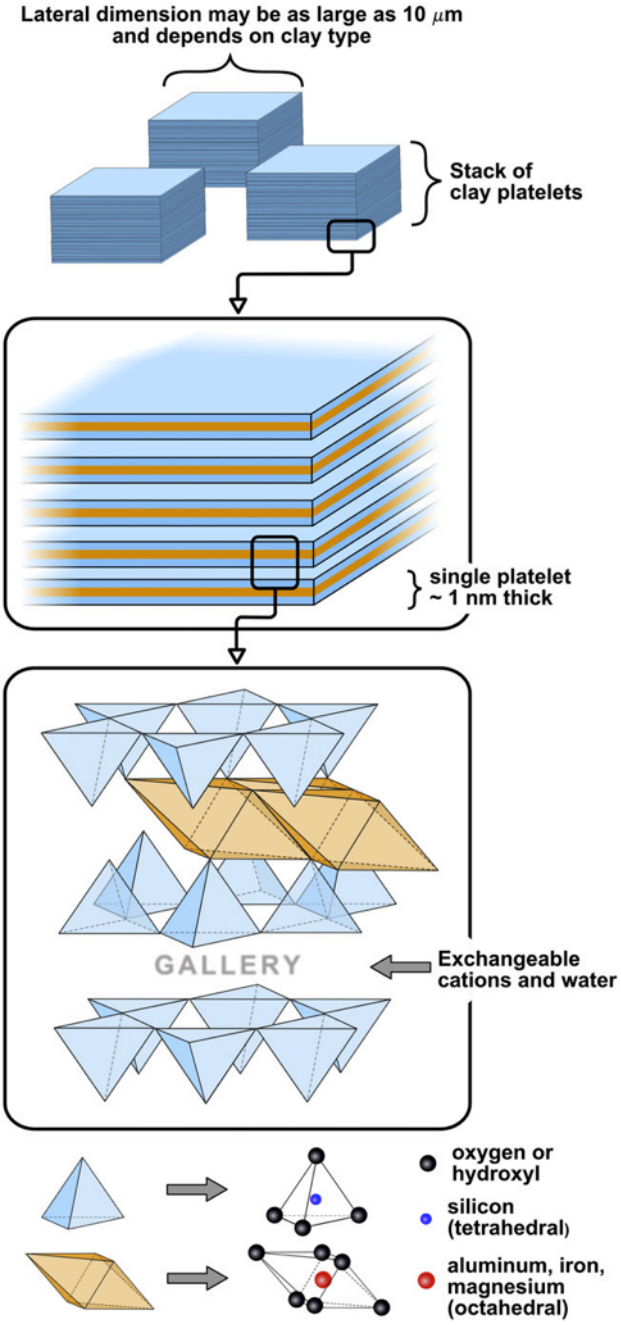

Figure 2.7 - Chemical and structural representation of montmorillonite [74].

Montmorillonite (MMT) is the most widely used clay for making polymer nanocomposites. This dioctahedral 2:1 phyllosilicate has silica tetrahedrons having oxygen and hydroxyl ions tetrahedrally arranged around central Si atoms. The aluminum octahedral sheet has Al^{3+} ion octahedrally coordinated to the hydroxyl groups. Two third of the Al^{3+} ions are substituted by lower valency cations such as Mg^{2+} and Fe^{2+} in octahedral sites [75, 76]. The difference in valences of Al, Mg and Fe creates negative charges distributed within the plane of the platelets that are balanced by positive ions, typically sodium ions, located between the platelets [15]. These clays present stacks of platelets, as showed in Figure 2.7, and an interlamellar space or gallery if about ~1 nm separates these platelets. MMT is white-pale yellow in color [74, 77].

Common clay minerals are hydrophilic and therefore incompatible with a wide range of hydrophobic polymers [78]. To overcome this restriction and to prevent aggregation, the clay surface is modified by exchanging the cations initially present in the interlayer with organic cationic surfactants, mainly primary, secondary, tertiary and quaternary alkylammonium or alkylphosphonium cations (Figure 2.8) [75, 79, 80].

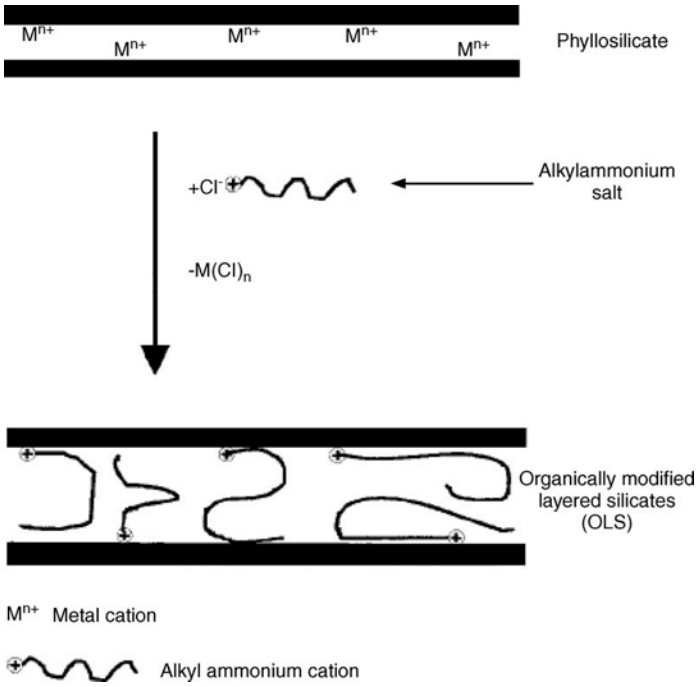

Figure 2.8 – Schematic demonstration of clay organic modification [75].

2.6.3. Synthesis of polymer nanoclay composites

At present there are three principal methods for producing polymer–layered silicate nanocomposites: *in situ* polymerization, solution processing and melt intercalation [81, 82].

In situ *polymerization* - in this method the nanoclay is dispersed in the monomer, which is then polymerized. The monomer may be intercalated with the help of a suitable solvent and then polymerized as illustrated in Figure 2.9. Polymerization can be initiated by heat or radiation, diffusion of a suitable initiator or catalyst fixed through cation exchange inside the interlayered before the swelling step [81, 83, 84].

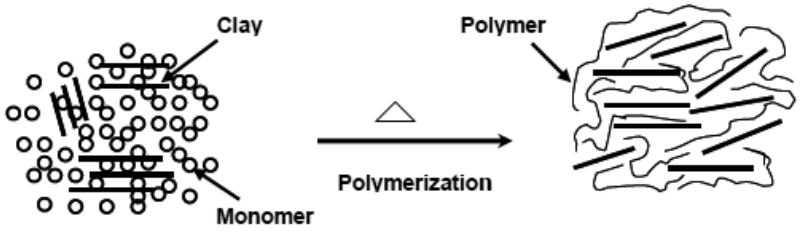

Figure 2.9 - Scheme of nanocomposite synthesis by in-situ polymerization [85].

Solution dispersion - is based on a solvent system in which the polymer is soluble and, at the same time, the nanoclays are able to swell. In general, the clays are first swollen in a solvent, such as water, chloroform or toluene, to form a homogeneous suspension in which the soluble polymer is successively added [30, 86]. The process ends with the evaporation of the solvent or the precipitation of the mixture, trapping the polymer chains intercalated into the galleries of the clays [83, 87].

This method is preferred for polymers that require high processing temperature at which the organoclay may degrade. Using this method, intercalation only occurs for certain polymer/solvent pairs [76]. This method is good for the intercalation of polymers with little or no polarity into layered structures and facilitates production of thin films with polymer-oriented clay intercalated layers [88]. However, from industrial point of view, this method involves the copious use of organic solvents, which is usually environmentally unfriendly and economically not viable [30].

Melt processing - this method involves the mixing of polymer with nanoclays above the polymer glass transition or melt temperature [87]. At higher temperatures polymer chains are sufficiently mobile to diffuse into the galleries of the clay (Figure 2.10) [86, 89]. Melt intercalation is an environmentally friendly technique, as it does not require any solvent. It is also commercially attractive due to its compatibility with existing processing techniques [76, 84]. This method was used to prepare the nanocomposites studied in this work.

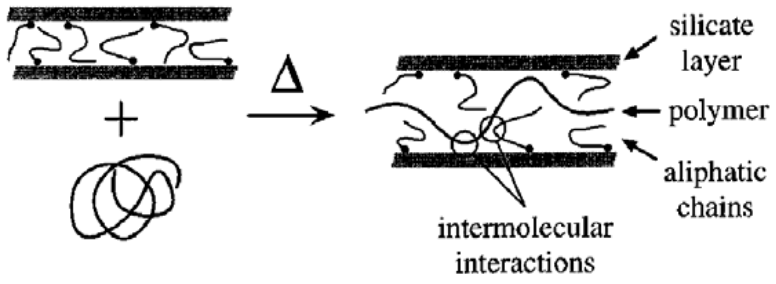

Figure 2.10 - Scheme of nanocomposite synthesis by melt processing [85].

Any physical mixture of a polymer with silicate (or inorganic material in general) does not necessarily form a nanocomposite [90]. Depending on the nature of components (polymer matrix, clay filler and organic surfactant) and processing conditions, clay particles can present different configurations when incorporated in the polymer matrix [75]. The literature commonly refers three types of morphology: immiscible (conventional or microcomposite), intercalated, and exfoliated. These are schematically illustrated in Fig. 2.11 along with example transmission electron microscopic (TEM) images and the expected wide angle X-ray scans (WAXS) [15].

Immiscible **–**in this case, the nanoclay platelets exist in particles comprised of stacks or aggregates of stacks more or less as they were in the clay powder, i.e., no separation of platelets. Thus, the wide angle X-ray scan of the polymer composite is expected to look essentially the same as that obtained for the organoclay powder [15].

Intercalated **–** intercalated structures are formed when a single (or sometimes more) extended polymer chain is intercalated between the silicate layers. The result is a well ordered multilayer structure of alternating polymeric and inorganic layers, with a repeat distance between them [86, 90]. In this case it is seen a peak shift in X-ray scans which indicates that the gallery has expanded, and it is usually assumed that polymer chains have entered or have been intercalated in the gallery [15].

Exfoliated **-** exfoliated structures are obtained when the clay layers are well separated from one another and individually dispersed in the continuous polymer matrix. In this case, the polymer separates the clay platelets and no peak is visible in the X-ray scans [90, 91].

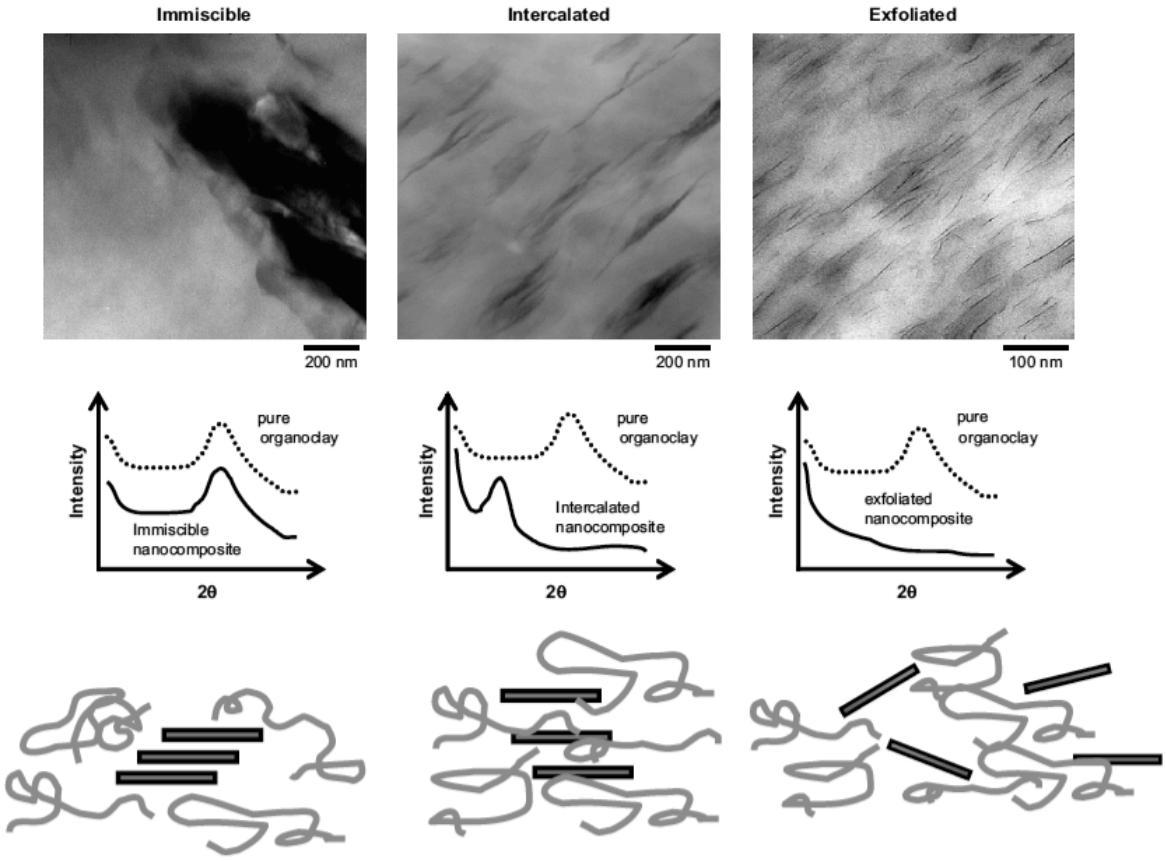

Figure 2.11 - Illustration of different states of dispersion of organoclays in polymers with corresponding WAXS and TEM results [15].

The exfoliated configuration is of particular interest because it maximizes the polymer–clay interactions making the entire surface of layers available for the polymer [69]. This should lead to the most significant changes in mechanical and physical properties. In fact, it is generally accepted that exfoliated systems give better mechanical properties than intercalated ones. However, it is not easy to achieve complete exfoliation of clays and, indeed with few exceptions, the majority of the polymer nanocomposites reported in the literature were found to have intercalated or mixed intercalated-exfoliated nanostructures [90].

Chapter 3

Experimental

"Nothing in life is to be feared, it is only to be understood. Now is the time to understand more, so that we may fear less."

— Marie Curie

In order to study thermal and UV stability of PLA with nanoclays incorporation, different nanocomposites were prepared. This chapter will be dedicated to the detailed description of the materials and the processing technique used in the preparation of PLA samples. Moreover, the equipment and experimental conditions used in these studies will be presented.

Afterwards, a concisely description of the characterization techniques employed on materials characterization and to follow thermal and photo-oxidative degradation of PLA and PLA nanocomposites will be made.

3.1. Materials

A commercial grade PLA (3251D) was supplied by NatureWorks LLC (USA). The three modified MTT used were supplied by Southern Clay Products (USA) – Cloisite 30B and Cloisite 15A – and by Laviosa Mineraria (Italy) – Dellite 43B. The characteristics of the used PLA and clays are listed in Table 3.1 and 3.2, respectively.

Table 3.1 – PLA properties.

Physical properties	
Specific gravity	1.24
Relative viscosity	2.5
Crystalline melt temperature (°C)	160-170
Glass transition temperature (°C)	55-65
Clarity	Transparent
Mechanical properties	
Tensile yield strength (MPa)	48
Tensile Elongation (%)	2.5
Notched Izod Impact (J/m)	16.0
Flexural strength (MPa)	83

Chloroform and deuterated chloroform (Table 3.3) were purchased from Lab-Scan and Acros Organics, respectively, and used as received.

Table 3.2 - Structure of nanoclays modifiers.

Commercial name	Modifier structure [a]	Extent of modification (meq/100 g clay)	% Moisture	% Weight loss on ignition	Code
Cloisite 30B	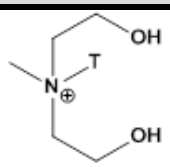	**90**	**< 2**	**30**	**C30B**
Cloisite 15A	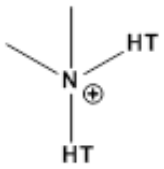	**125**	**< 2**	**43**	**C15A**
Dellite 43B	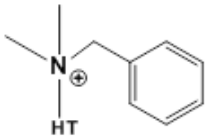		**3 (max)**	**32 - 35**	**D43B**

[a] T is tallow (~65% C18; ~30% C16; ~5% C14)

Table 3.3 - Characteristics of the used reagents.

Solvent	Molecular formula	Molecular weight (g/mol)	Density (g/cm^3)	Risk statements	Safety statements	Purity
Chloroform	$CHCl_3$	119.38	1.489	22-38-40 48/20/22	36/37	99.5%
Chloroform-d	$CDCl_3$	120.39	1.500	22-38-40 48/20/22	36/37	99.8% d-enrichment

3.2. Samples preparation

Polymer pellets and modified MMT were dried in a vacuum oven at 60 °C for 12 h before use. PLA nanocomposites with 3 and 5 wt.% of C30B, C15A and D43B were prepared, after pre-mixing, in a Haake batch mixer (HAAKE Rheomix 600 OS; volume 69 mL) equipped with two rotors running in a counter-rotating way and the weight (g) used in each case is listed in Table 3.4. The rotor speed was 80 rpm, the set temperature was 190 °C and the mixing time was 5 minutes.

Table 3.4 – Materials weight for Haake preparation.

Nanoclay incorporation (wt.%)	Nanoclay (g)	PLA (g)
0	-	58.00
3	1.74	56.26
5	2.90	55.10

The prepared nanocomposites were pressed into thin films and thick discs at 200 °C under 30 ton for 60 s. The thickness of each film (ca. 40 μm) was measured with a pachymeter Mitutoyo.

3.3. Degradation

3.3.1. Thermo-oxidative degradation

In order to evaluate the thermo-oxidative stability of PLA and PLA nanocomposites, samples were subjected to constant heat at 140°C for 120 hours in a Heraeus vacutherm oven under air (Figure 3.1). The experiments were carried out on small rectangular sections of the thin films and samples were taken along time to be characterized.

Figure 3.1 – Representation of the used oven on thermal degradation.

3.3.2. Photo-oxidative degradation

The accelerated weathering of PLA and PLA nanocomposites were carried out in a XenoTest 150 S chamber from Heraeus (Original Hanau) according to the ISO 4892-2. The XenoTest 15 S is equipped with: a Xenon light source with an intensity of 60 Wm^{-2}; optical filter system (according to Figure 3.2); humidification unit; distilled water vessel; pump and piping system for circulation of the water to the humidification and rain sprain units; and 10 specimen holders (dimensions of 135 x 45 mm), with double face, in vertical position and mounted on a revolving cylindrical rack which is rotated around the light source. The holders also turn on their own axis (rotational) simulating dark/light cycle.

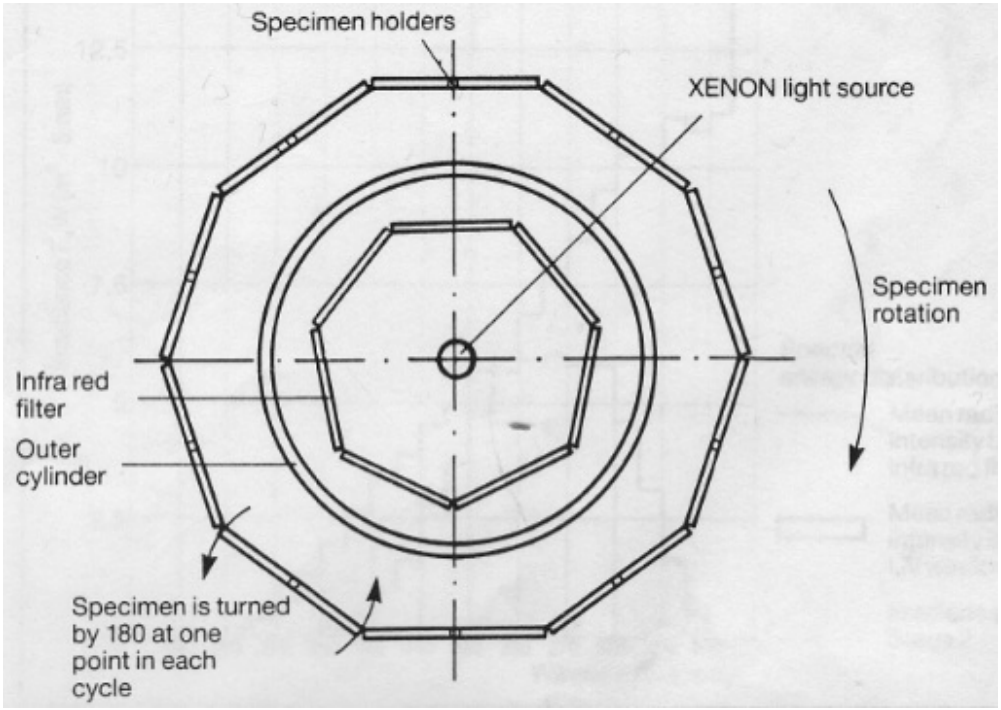

Figure 3.2 – Arrangement of optical filter system and specimen holders in accelerated chamber.

The light of the xenon lamp was filtered under 300 nm (Figure 3.3) with an UV window combined with six IR filter glasses and a dark UV filter glass. The XenoTest creates an accelerated environment of the natural weathering conditions, simulating materials behaviour during its lifetime, i.e., daylight exposure with heat, oxygen and humidity. The accelerated weathering conditions are listed in Table 3.5.

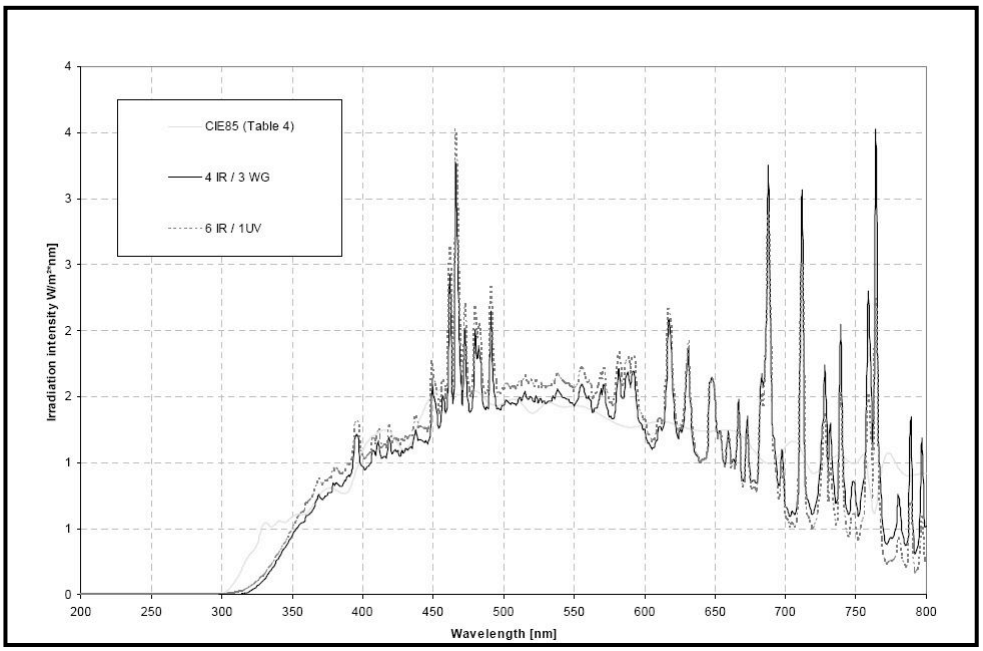

Figure 3.3 - Spectral energy distribution in wavelength range of 200-800 nm.

Samples were removed after 100, 200, 300, 400, 500 and 600 hours of exposure and characterized by several analytical techniques.

Table 3.5 - Conditions in accelerated weathering chamber.

Cycle period	Cycle time (minutes)	Temperature (ºC)	Relative humidity (%)
Rain	18	23.0	85.0
Dry	102	30.0	58.0

3.4. Materials characterization

3.4.1. Scanning Electron Microscopy (SEM)

The scanning electron microscope is one of the most versatile instruments available for the examination and analysis of the microstructural characteristics of solid materials [92]. SEM permits the observation and characterization of heterogeneous organic and inorganic materials on a nanometer (nm) to micrometer (μm) scale and became particularly important in the study of micro and nanomaterials [93]. In this technique electrons from a thermionic cathode are accelerated and hit the surface of the sample yielding secondary electrons and backscattered electrons, used for the image, Auger electrons and X-ray radiation [94, 95]. SEM is used to examine the surface of polymers and can reveal morphological changes under the action of influencing

parameters, such as different preparation conditions, outdoor weathering and physical and thermal ageing [93, 96]. Another important aspect, which is more related to nanocomposites, is the dispersion state of the nanoparticles in the polymeric matrix and SEM may additionally play a significant role, particularly to examine the presence of agglomerates [97, 98].

An energy-dispersive spectrometer (EDS) can be coupled to the SEM to detect characteristic X-rays of all elements above atomic number 4. The EDS system offers an evaluation on the elemental constitution of a sample [92].

The prepared nanocomposites with different wt.% of nanoclay incorporation were fracture in liquid nitrogen, fixed with a conducting bi-adhesive tape on aluminium stubs and gold plating. The morphology of the samples was studied using a Leica Cambridge S360 scanning electron microscope.

In order to evaluate qualitatively the elemental constitution of the different nanoclays used in this work, powder samples were analysed by EDS in the same SEM equipment.

3.4.2. Fourier Transformed Infrared spectroscopy (FTIR)

An infrared absorption spectrum of a material is obtained simply by allowing infrared radiation to pass through the sample and determining what fraction is absorbed at each frequency within some particular range. The frequency at which any peak in the absorption spectrum appears is equal to the frequency of a vibration mode of the molecules of the sample [8]. This method is rapid and sensitive, not expensive and with sampling techniques that are easily used [99].

This analytical technique as been used to identify and characterize polymers, as it can provide information about chemical structure and the presence of additives and impurities. In the case of nanocomposites, FTIR is used to analyse the interactions between the polymer and the filler used. FTIR also allows to follow the thermal and photo-degradation of polymers, identifying the structural changes that occur throughout degradation [8, 100].

Room temperature infrared spectra of the initial and degraded films of all prepared samples and nanoclays powders (pressed into pellets with 2 % of nanoclay and 98 % of KBr) were recorded on an ABB FTLA 2000 spectrometer in the range 4000-500 cm^{-1} by averaging 16 scans and using a resolution of 4 cm^{-1}.

3.4.3. X-ray Diffraction (XRD)

XRD is a powerful technique that operates by directing an incident ray beam to a sample, which is then diffracted at specific angles and intensities depending on the

crystalline and amorphous phases of the sample. Through the analysis of XRD, valuable information of polycrystalline materials can be obtained like the identification of the crystalline phases present in materials and measurement of the structural properties, such as grain size and preferred orientation [101]. In the case of nanocomposites characterization, XRD results give an indication of the dispersion morphology of the nanoparticles and the interlayer spacing (a few angstroms in size) can also be determined [102, 103].

The diffraction patterns were obtained using a diffractometer (AXS Nanostar-D8 Discover, Bruker) equipped with a CuKα generator (λ = 1.5404 Å) at 40 kV and 40 mA, in a 2θ range from 0.08 – 10°. The nanoclays were analysed directly, whereas the nanocomposite samples were previously compression molded into disks with a diameter of 20 mm and a thickness of 4 mm.

3.4.4. Nuclear Magnetic Resonance spectroscopy (NMR)

NMR is a dominant analytical tool, which has widespread applications in all areas of synthetic chemistry and can provide accurate qualitative and quantitative information on the chemical structure of the analysed compounds [8]. The fundamental property of the atomic nucleus involved in NMR is the nuclear spin, *I*, which must be a value that proportionate the nucleus to have a magnetic moment. The nuclei commonly observed in NMR spectroscopy of organic compounds (^{1}H and ^{13}C) have spin $I=½$ [104]. When applied to polymers, NMR give information about chemical structural and is also capable of providing detailed information on certain aspects of chain structure which are not accessible by other techniques [105, 106].

^{1}H NMR spectra of initial and degraded PLA and PLA nanocomposites with 3 wt.% nanoclay incorporation were recorded on a Varian Unity Plus 300 MHz spectrometer using deuterated chloroform as solvent and tetramethylsilane as internal standard.

3.4.5. Viscosity measurements

Polymer molecules possess the unique capacity to greatly increase the viscosity of the liquid in which they are dissolved, even when present at low concentrations [107] and the measurement of the viscosity of dilute solutions is the oldest, simplest and most widely used method for obtaining information about the molecular weight of a polymer. Determination of the intrinsic viscosity requires the measurement of the viscosities of several dilute solutions [108]. A large number of sophisticated viscometers exist for the accurate measurement of solution viscosity and its variation with concentration, shear rate and temperature. Figure 3.4 shows an Ubbelohde capillary viscometer and when in use, the bulb A is filled with a solution of known concentration. A volume V of this

solution is then transferred to completely fill bulb C between marks E and F by closing arm N and applying a pressure down arm L. Further draining of liquid out of bulb C is prevented by closing arm M, and the viscometer is transferred to a thermostatted bath. On simultaneously opening N and releasing the pressure in L, excess liquid drains back into A, leaving bulb C filled. The time taken for the liquid level to move from mark F to mark E is recorded and the process is then repeated for the pure solvent and also for the polymer solutions [5].

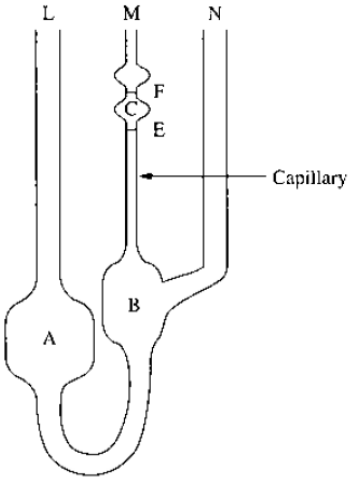

Figure 3.4 - Representation of an Ubbelohde capillary viscometer [5].

The intrinsic viscosity (η) of all samples (initial and degraded) was determined using an Ubbelohde capillary viscometer, represented in Figure 3.5, with 5 mg ml^{-1} solutions in chloroform at 25.0 ± 0.5 °C and according to the following equation [45]:

$$\eta = \frac{\sqrt{2((\eta_r - 1) - \ln \eta_r)}}{c} \qquad \text{(eq. 1)}$$

where η_r is relative viscosity and c is polymer solution concentration.

Five measurements were performed and averaged to obtain the solution viscosity of each sample.

Figure 3.5 – Representation of the equipment used to measure the intrinsic viscosity.

3.4.6. Thermogravimetric Analysis (TGA)

Thermogravimetry evaluates the mass change of a sample as a function of temperature or time (in the isothermal mode) as the specimen is subjected to a controlled temperature program in a controlled atmosphere [109]. Not all thermal events bring a change in the sample mass (for example melting, crystallization or glass transition), but there are some very important exceptions, which include desorption, absorption, sublimation, vaporization, oxidation, reduction and decomposition. TGA is used to characterize the decomposition and thermal stability of materials, including polymers and polymeric materials, under a variety of conditions, and to examine the kinetics of the physical-chemical processes occurring in the sample [110].

Thermogravimetric analyses of PLA and PLA nanocomposites with 3 wt.% of nanoclays addiction were performed using a TGA Q500 (TA Instruments) at 10 °C/min from 30 to 500 °C under nitrogen flow. Initial sample weight was approximately 10 mg.

3.4.7. Differential Scanning Calorimetry (DSC)

The differential scanning calorimeter is perhaps the instrument that has dominated the field of thermal analysis in the past decade [111]. In a DSC experiment the difference in energy input to a sample and a reference material is measured while the sample and reference are subjected to a controlled temperature program [109, 112]. Such measurements provide quantitative and qualitative information about physical or chemical changes that involves exothermic and endothermic processes or changes in heat capacity [113]. DSC can provide information on: glass transition; melt point; crystallisation time and temperature; crystallinity; oxidative stability; polymer heat history studies; reaction kinetics; thermal stability, among others [113].

Thermal properties of initial and degraded PLA and PLA nanocomposites with 3 wt.% nanoclay were determined in a Perkin-Elmer DSC 7 under nitrogen. Approximately 6 mg of each sample were cut from the films and placed in an aluminum pan. The analysis was performed in three steps: first heating from 30 to 250 °C at 50 °C/min, cooling from 250 to 30 °C at 10 °C/min, and second heating from 30 to 250 °C at 10 °C/min. Two minute isothermal plateau were inserted between the ramps. The melting and glass transition temperatures (T_m and T_g respectively) were obtained and degree of crystallinity (χ) was determined using the melting enthalpy for PLA of 100% crystallinity (ΔH_m^0= 146.0 J g^{-1}) [25] according to the following equation:

$$\chi(\%) = \frac{\Delta H_m}{\Delta H_m^0} \times 100 \qquad \text{(eq. 2)}$$

where ΔH_m is the experimental melting enthalpy obtained for the samples.

Chapter 4

Results and Discussion

"The most exciting phrase to hear in science, the one that heralds the most discoveries, is not "Eureka!" (I found it!) but 'That's funny..."

— Isaac Asimov

In this chapter the results obtained are presented and discussed, but for a better understanding, they were divided in three subchapters: materials characterization, thermo-oxidative degradation and photo-oxidative degradation.

The first subchapter presents results from characterization of the initial materials used and the PLA and PLA nanocomposites prepared by melt mixing.

The second and third subchapters present the results concerning the thermal and photo-oxidative degradation, respectively.

4.1. Materials Characterization

4.1.1. EDS analysis of nanoclays

As it was said before, thermal degradation of PLA is influenced by the presence of residual metals as they can lower the thermal degradation temperature and induce the remarkable racemization of lactic acid monomeric unit [47].

According to Tian et al. [114], MMT is constituted by 58 % of SiO_2, 22 % Al_2O_3, 3 % of MgO and Na_2O, 2 % of Fe_2O_3 and also present CaO, K_2O and trace amounts of TiO_2 and MnO. The nanoclays used in this work were analysed by EDS to obtain information about their elemental constitution, specially the presence of metals that have influence on thermal degradation of PLA. Figure 4.1 presents the EDS results for the powder of C30B and Table 4.1 the relative % of some elements of all clays.

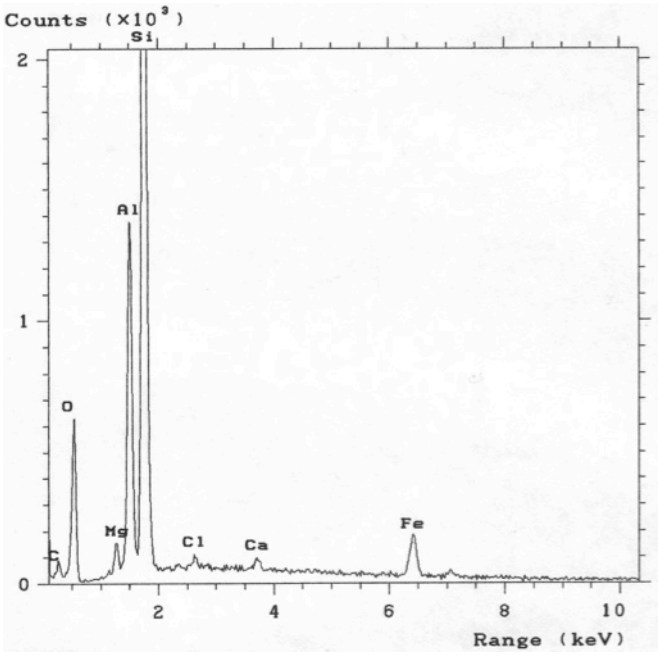

Figure 4.1 – EDS results for C30B powder.

As EDS only provides qualitative elemental information, the results obtained cannot be compared with the ones from the literature. However, it is possible to see that there are no significant differences between the relative percentages of the nanoclay elements that could influence thermo-oxidative degradation of PLA.

Table 4.1 - Elemental constitution of the nanoclays used.

Nanoclay / Element (relative %)	C30B	C15A	D43B
Mg	3.0	2.9	3.0
Al	24.1	24.1	22.8
Fe	5.0	4.5	4.5
Ca	0.8	0.4	0.8

4.1.2. Chemical structure analysed by NMR

NMR is the most effective available technique for determining chemical structures and is routinely employed to characterise and to identify the chemical structures present in polymers. PLA was analysed by ^{1}H-NMR spectroscopy and the spectra is represented in Figure 4.2.

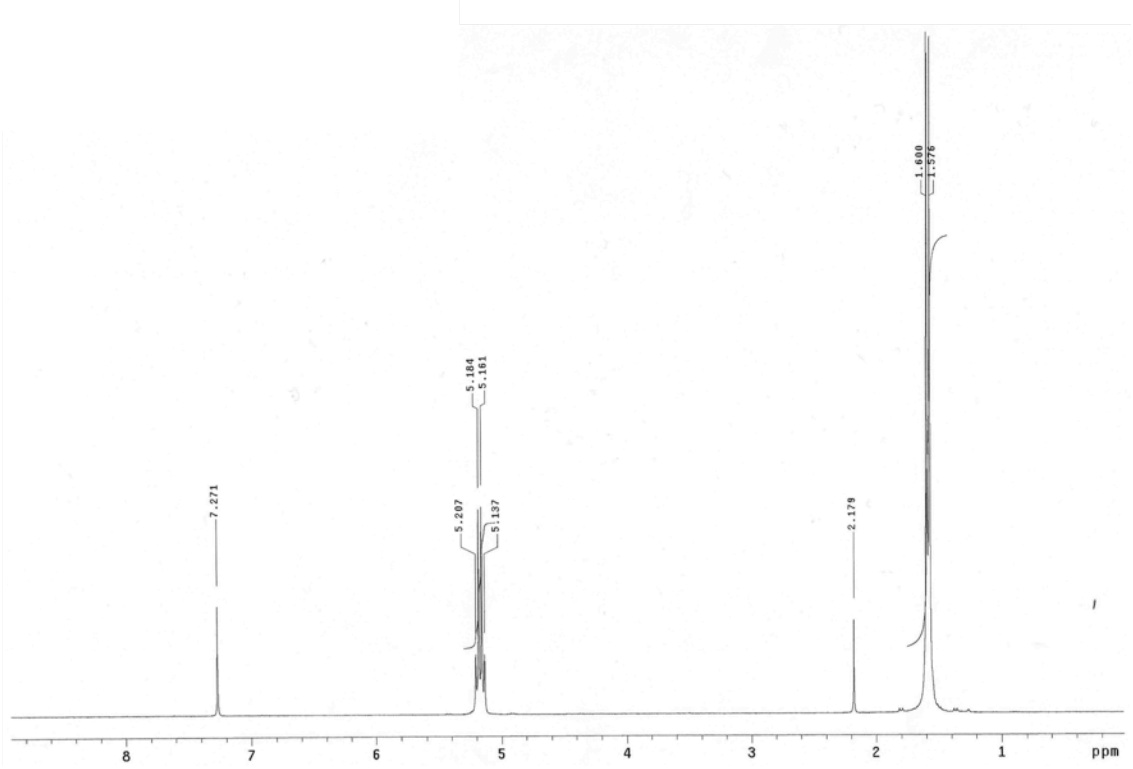

Figure 4.2 - ^{1}H NMR spectra of PLA.

The characteristic peaks of PLA at chemical shift (δ) 5.16 and 1.57 ppm are respectively ascribed to –CH and $–CH_3$ protons of PLA repeat unit and this assignments are in well agreement with literature [115]. The resonance peaks at 7.27 and 2.17 ppm correspond respectively to the residual solvent ($CDCl_3$) and to acetone used in the wash of the material.

The prepared nanocomposites were also analysed by ^{1}H-NRM and the results were equal to PLA (results not shown).

4.1.3. Chemical structure analysed by FTIR

Infrared is an important analytical technique used to identify and characterize polymers as it provides information about their chemical structure. In figure 4.3 a) and b) is presented the FTIR spectra of PLA recorded in two different regions, i.e., 4000-2500 and 1900-500 cm^{-1}. In the first region are observed bands assigned to OH and to CH stretch. The second region exhibits bands assigned to C=O, CH, CC and COC. The compilation, comparison with reference works and attributions of these bands are listed in Table 4.2 and it is seen that all bands are in concordance with references [88, 115-121].

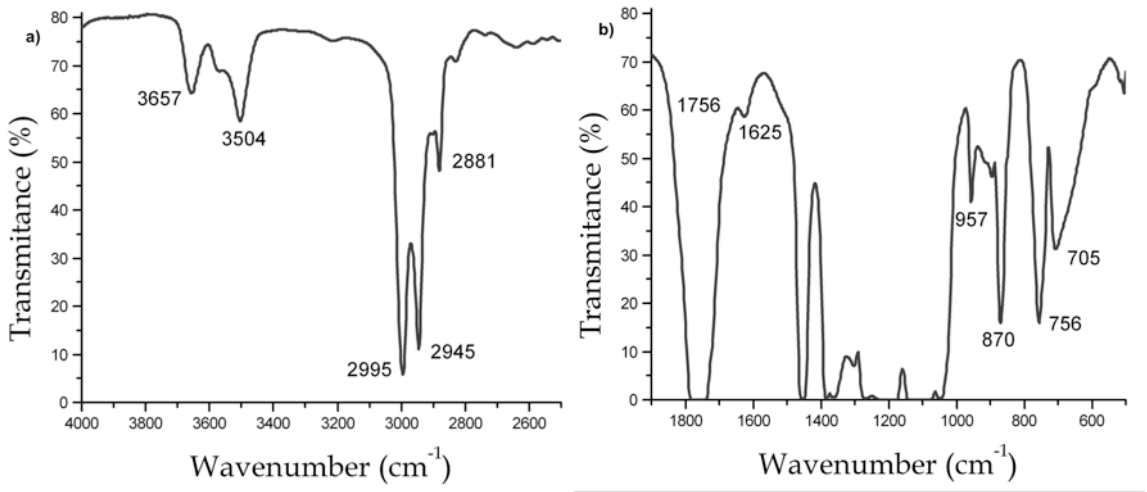

Figure 4.3 - FTIR spectra of PLA in two regions: a) 4000-2500 cm^{-1} and b) 1900-500 cm^{-1}.

Table 4.2 - Attribution of the principal FTIR bands of PLA

Experimental bands (cm^{-1})	Reference bands (cm^{-1})	Assignments [a]	Reference
3657	3658	ν OH	[88, 119]
3504	3504	ν OH	[115, 120]
2995	2995	ν_{as} CH_3	[115, 116, 120]
2945	2945	ν_s CH_3	[115, 116]
2881	2882	ν CH	[115, 116]
1756	1760	ν C=O	[115-118]
1625	1618	OH (water)	[119]
1450 - 1460	1452	δ_{as} CH_3	[115, 117]
1350 – 1400	1348 - 1388	δ_s CH_3 + δ CH	[116, 120]
1160 - 1290	1270 1215 - 1185 1190 - 1186	δ CH + ν COC ν_{as} COC + ν_s COC ν_{as} COC + γ_{as} CH_3	[115, 116]
1045 - 1150	1130 1100 1045	γ_{as} CH_3 ν_s COC ν C-CH_3	[115, 116, 121]
957	955	γ CH_3 + ν CC amorphous phase	[115, 118]
870	867	ν C-COO amorphous phase	[58, 115, 121]
756	760-740 755	δ C=O crystalline phase	[116] [88, 115]

[a] ν = stretching vibration; ν_{as} = asymmetric stretching vibration; ν_s = symmetric stretching vibration; δ = bending vibration ; δ_{as} = asymmetric bending vibration; δ_s = symmetric bending vibration; γ = out-of-plane bending vibration; γ_{as} = asymmetric out-of-plane bending vibration.

FTIR was also used to characterize the interactions between PLA and nanoclays in the nanocomposites with different wt.% of nanoclay incorporation. Figure 4.4 a), b) and c) shows the FTIR spectra of PLA, nanoclays and nanocomposites with different wt.% incorporation of C30B, C15A and D43B. Analysing the FTIR spectra of the three nanoclays it is possible to identify characteristic bands: bands around 3500 cm^{-1} assigned to OH stretch, 2940 and 2880 cm^{-1} associated with CH stretch, 1472 and 726 cm^{-1} assigned to CN stretch of the organo-modifiers and at about 950-1050 cm^{-1} SiOSi stretching [88, 122, 123].

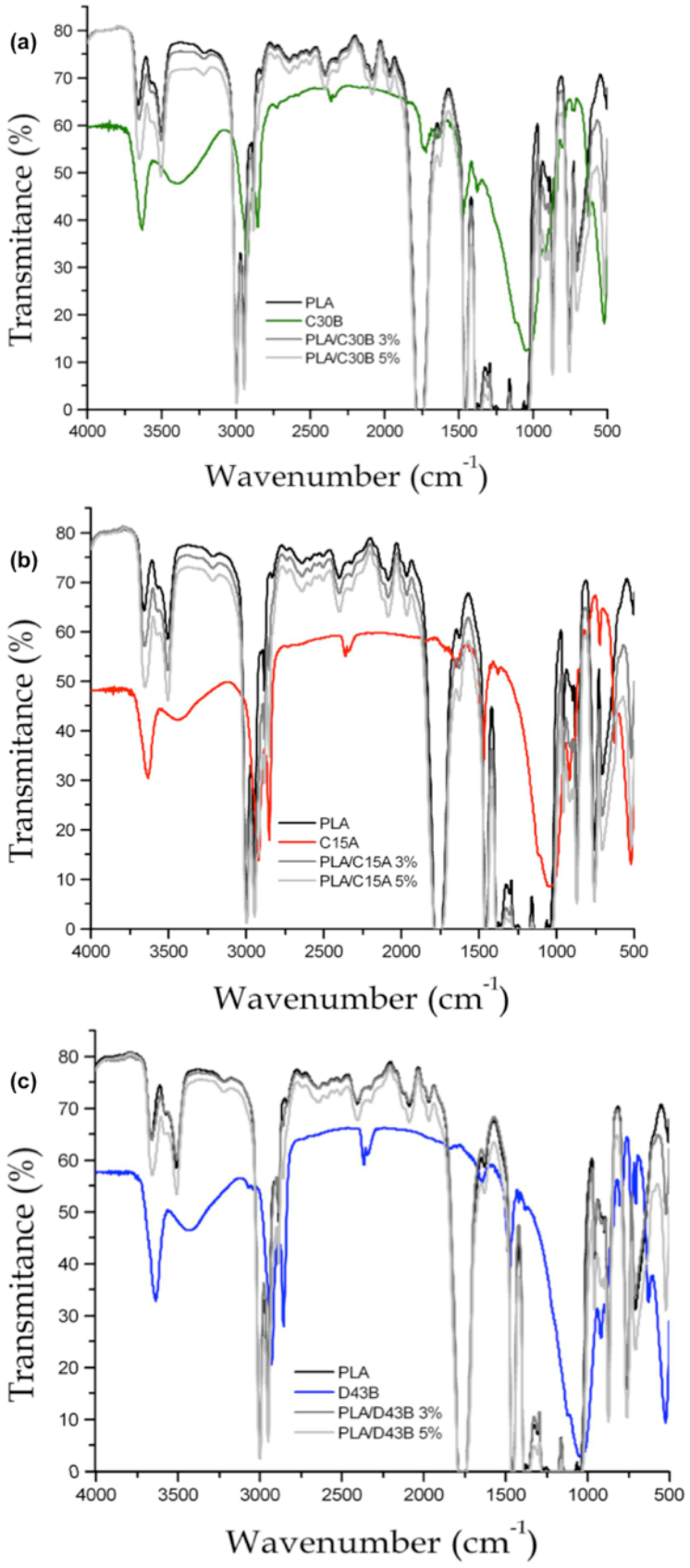

Figure 4.4 - FTIR spectra of PLA, nanoclays and PLA nanocomposites with different wt.% nanoclay incorporation: a) C30B, b) C15A and c) D43B.

Comparing the FTIR spectra of PLA with PLA nanocomposites (Figure 4.4), no significant changes are observed as a result of the nanoclays addition. Some nanoclay bands are covered by the saturation of the PLA bands and is only noted a little increase intensity in some common bands (this increase is higher for nanocomposites with 5 wt.% nanoclay incorporation). Although the organo-modifiers of the nanoclays are different, infrared spectra are similar between all nanoclays and nanocomposites.

4.1.4. Study of nanocomposites morphology

SEM is a technique widely used to study materials morphology and Figure 4.5 shows the fractured surface of PLA nanocomposites with 3 and 5 wt.% of nanoclay incorporation.

A good dispersion degree of nanoclay particles without aggregates in the micron range can be observed in the micrographs of the samples containing 3 and 5 wt.% of PLA/C30B and 3% of PLA/D43B. Contrarily, the sample with 5 wt.% of D43B exhibits some clay aggregates dispersed in the polymer matrix. The incorporation of 3 and 5 wt.% of C15A results in worse level of clay dispersion since more clay aggregates were observed.

The better dispersion achieved with C30B can be associated to the strong interactions between the carbonyl functions of PLA chains and hydroxyl functions of C30B, which seem to improve the dispersion of this clay in the PLA matrix [64, 124].

Based on morphology and nanoclay dispersion, most of the future analyses performed and presented in this thesis were made with nanocomposites with 3 wt.% nanoclays incorporation.

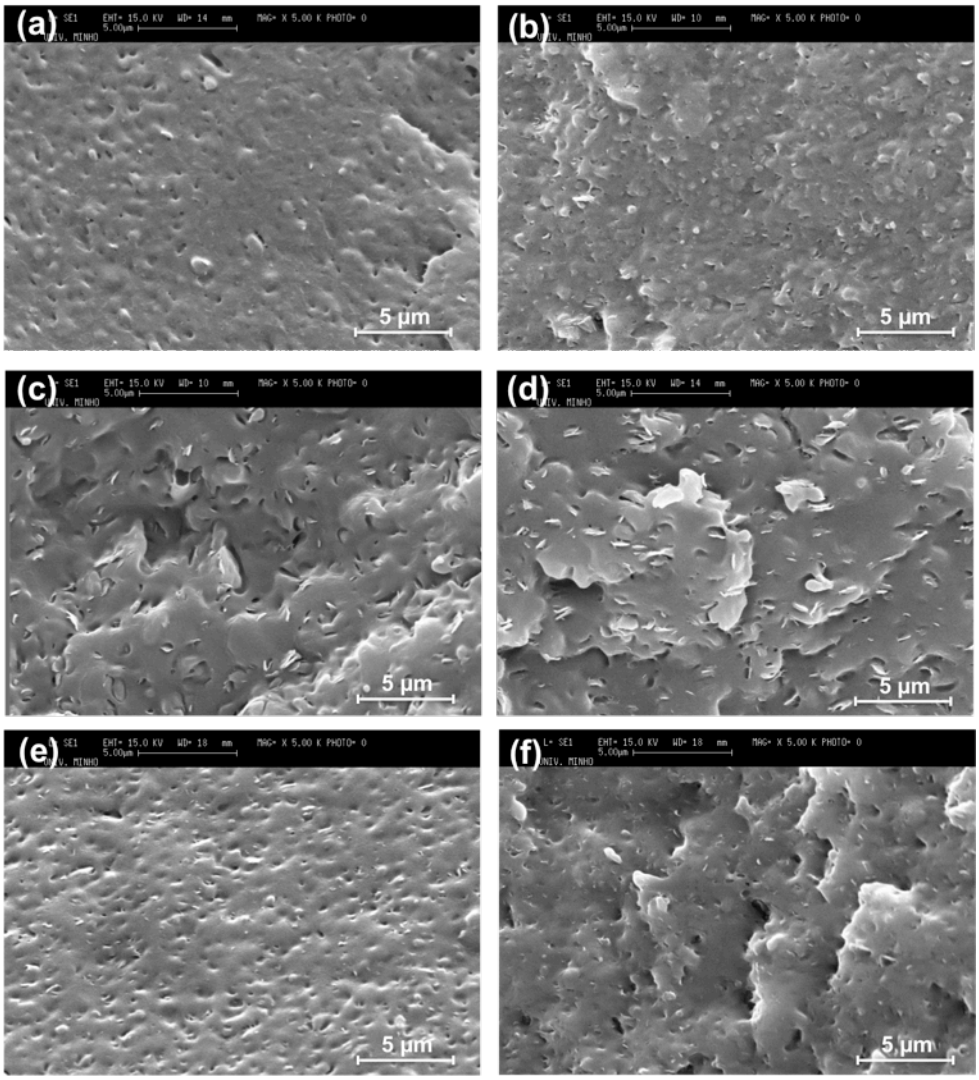

Figure 4.5 - SEM micrographs of (a) PLA/C30B 3 wt.%, (b) PLA/C30B 5 wt.%, (c) PLA/C15A 3 wt.%, (d) PLA/C15A 5 wt.%, (e) PLA/D43B 3 wt.% and (f) PLA/D43B 5 wt.%.

4.1.5. Study of nanoclays dispersion

XRD is one of the most common techniques used to analyze nanocomposite structure. The position, shape, and intensity of the different peaks may allow to evaluate the dispersion of mineral sheets within the polymer matrix [121, 125].

Figure 4.6 shows the XRD patterns of the nanoclays used and PLA nanocomposites with 3 wt.% nanoclay incorporation.

Compared with powder nanoclays, the diffraction peak (001) plane in the nanocomposites shifts to lower angles. The decrease of the diffraction angles means that PLA macromolecules were inserted between the nanoclay layers and nanocomposites with an intercalated structure were obtained. The d-spacing values (basal distance between clay layers) were calculated using Bragg's law ($\lambda = 2d\sin\theta$; d is the interlayer d-spacing and λ is the wave length). The calculated d_{001} distance expands 1.60 nm for

PLA/C30B, 0.62 nm for PLA/C15A and 0.38 and/or 1.65 nm for PLA/D43B (Figure 4.6 (a), (b) and (c), respectively). According to these results, while nanocomposites with C30B present higher increase of interlayer separation, nanocomposites with C15A show lower.

From XRD results little can be said about the spatial distribution of the nanoclays or any structural non-homogeneity in nanocomposites. In fact, SEM results indicate that clay aggregates were formed in PLA/C15A nanocomposites.

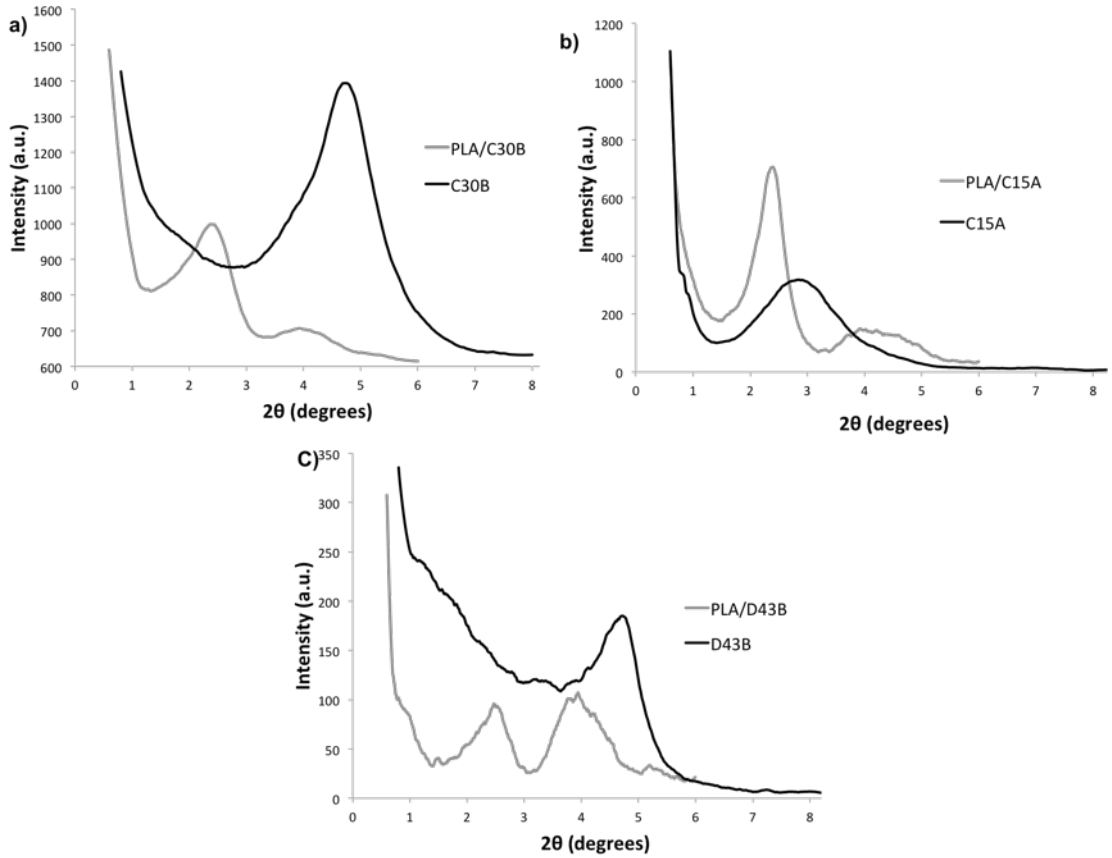

Figure 4.6 - X-ray diffractograms recorded for powder nanoclays and prepared nanocomposites of a) C30B, b) C15A and c) D43B.

4.1.6. Determination of intrinsic viscosity

The viscosity determination of a polymeric solution is a simple way to estimate and follow molecular weight changes of polymers.

Intrinsic viscosity (η) measurements were performed in PLA pellets and PLA and PLA nanocomposites prepared to evaluate the influence of processing and nanoclay incorporation. Figure 4.7 present the percentage of η difference between PLA pellets and PLA and PLA nanocomposites prepared by melt mixing. A decrease of 6 % in η was observed to PLA and is attributed to traces of residual monomers, water and residual

organometallic compounds used in the polymerization reactions, which can be responsible for the occurrence of chain length reduction by hydrolysis or alcoholysis reactions [126]. A very high sensitivity of PLA to thermal degradation during melt processing has been reported even in the presence of antioxidant [67]. After nanoclay incorporation a decrease in η was observed for all nanocomposites (8 % for C30B, 14-19 % for D43B and 20 % for C15A). This can be explained by the shear during melt mixing of PLA and nanoclay. Hydrolysis of the PLA matrix is accelerated by the high temperature, shear and the reactive groups of the modifiers of each clay [121]. C30B is the nanoclay that has less influence on thermal stability of PLA during processing (when compared with the other nanoclays studied in this work).

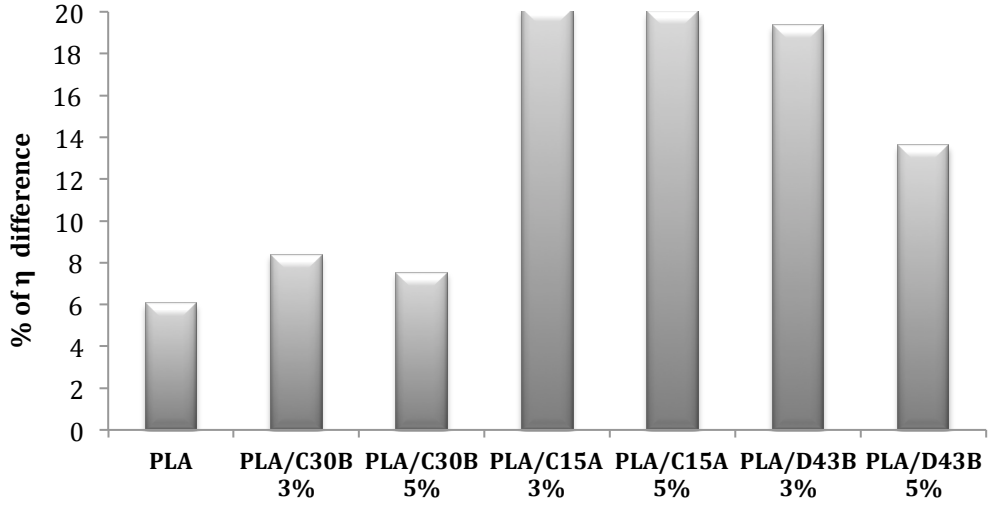

Figure 4.7 - % of η difference between PLA pellets and PLA and nanocomposites prepared by melt mixing.

4.1.7. Thermal analysis

TGA is used to evaluate the thermal stability of polymeric materials under different conditions. Thermal stability of PLA and PLA nanocomposites with 3 wt.% nanoclays incorporation was measured on TGA under nitrogen and the results are shown in Figure 4.8.

Results show that PLA has an onset degradation temperature of 331 °C, nanocomposites with C30B and C15A have 339 °C and with D43B this temperature is shifted to 341 °C. The incorporation of nanoclays in PLA matrix seems to increase the thermal stability of the polymer. It is generally believed that the introduction of inorganic components into organic materials can improve their thermal stabilities [121]. In nanocomposites with 3 wt.% nanoclay incorporation the increase in the thermal stability can be attributed to an ablative reassembling of the silicate layers, which may occur on the surface of the nanocomposites creating a physical protective barrier and,

on the other hand, volatilization might also be delayed by the effect of the silicate layers dispersed in the nanocomposites [25, 123, 127].

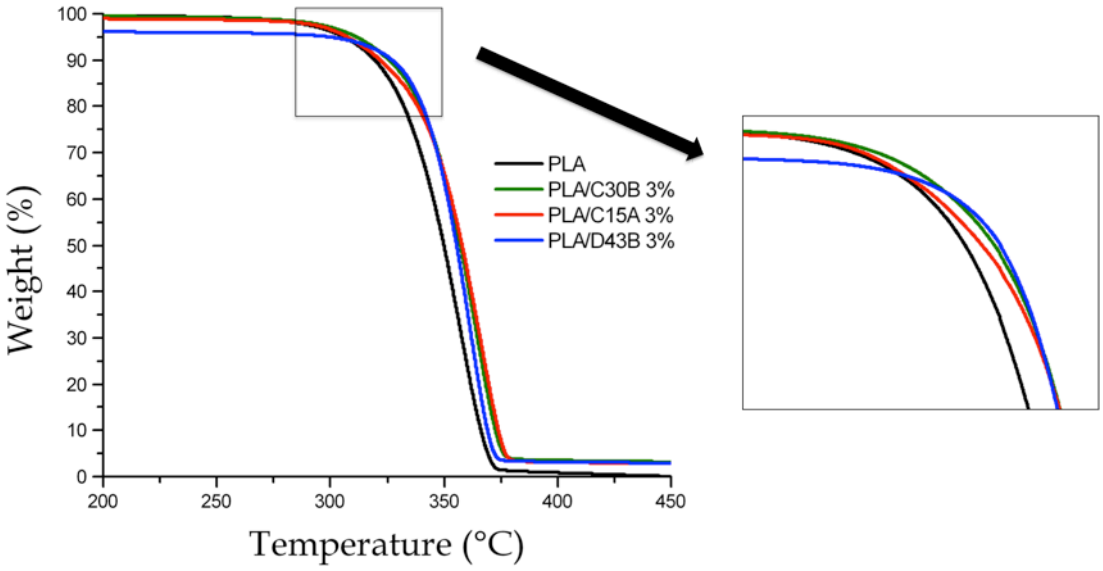

Figure 4.8 - TGA curves of PLA and PLA nanocomposites.

All nanocomposites present a final residue of 3% due to the presence of the nanoclays.

4.2. Thermo-oxidative degradation

After preparation and initial characterization, PLA and PLA nanocomposites were submitted to thermo-oxidative degradation as described in Experimental Chapter (3.3.1). The degraded samples were then analysed by NMR, FTIR, viscosimetry and DSC and the results compared with the ones obtained for initial samples.

4.2.1. ^{1}H NMR analyses

^{1}H NMR spectra were performed for PLA and PLA nanocomposites with 3 wt.% of nanoclay incorporation after 120h of thermo-oxidative degradation. The chemical shift (δ) values obtained in the ^{1}H-NMR spectra, signal intensities and the corresponding groups are listed in table 4.3. It was already observed that the assignments obtained for initial PLA and PLA nanocomposites were in well agreement with literature [115] and the results for degraded samples were similar (no changes in chemical shift values were observed). However, differences in the signal intensities can be noticed. The proton intensity ratio (CH_3/CH) has a theoretical value of 3 and this ratio must remain constant if degradation takes place upon the ester linkage, or if is processed by hydrolysis or

radical degradation, among others [128]. The proton intensity ratio for PLA 0h is 3.71 and for PLA 120h is 2.97, for PLA/C30B 0h is 3.22 and for C30B 120h is 3.07.According to the literature [128] only pyrolytic elimination (which is responsible for the transformation of $CH\text{-}CH_3$ into $CH{=}CH_2$) can be responsible for a lower ratio. But this mechanism, if present, must be a secondary and less important degradation pathway since there was no signal for CH_2 protons in ^1H NMR. Comparing PLA and PLA/C30B samples, the decrease of proton intensity ratio is higher for PLA, which can be related with different extent of thermal degradation. The results obtained for PLA/C15A and PLA/D43B (not shown) were similar to PLA/C30B.

Table 4.3 - ^1H NMR data for PLA samples.

	δ CH_3 (ppm)	Signal intensity (%)	δ CH (ppm)	Signal intensity (%)
PLA 0h	1.56 – 1.60	78.76	5.14 – 5.21	21.24
PLA 120h	1.58 – 1.60	74.81	5.13 – 5.21	25.19
PLA/C30B 0h	1.57	76.29	5.16	23.71
PLA/C30B 120h	1.57	75.43	5.15	24.57

4.2.2. Intrinsic viscosity measurements

The intrinsic viscosity (η) of PLA and its nanocomposites with 3 and 5 wt.% nanoclay addictions before and after 120 hours of thermo-oxidative degradation is depicted in Figure 4.9. Compared with initial values, a significant decrease in viscosity after 120 hours of degradation can be noticed for all samples. However, with the incorporation of 3 wt.% of nanoclays this decrease was lower than for PLA. Comparing these samples, the sequence of the viscosity decrease was the following: PLA > C30B > C15A > D43B. The incorporation of 5 wt.% of the nanoclays leads to a higher decrease in viscosity of PLA nanocomposites than PLA and than PLA with 3 wt.% but the trend is the same.

Since the intrinsic viscosity difference between initial and degraded PLA/D43B nanocomposites was lower than with the other nanoclays, it seems that the addition of D43B has more influence enhancing the PLA thermal stability, as it was already observed on TGA results. A possible explanation for this different behaviour between the different nanoclays can be the presence of hydroxyl groups in the chemical structure of C30B, associated to the good clay dispersion achieved (Figure 4.5), that could promote the hydrolysis of PLA macromolecules [129] resulting in a higher decrease of

intrinsic viscosity when compared to D43B. Since C15A and D43B do not have reactive chemical groups that could induce chain scission, the samples with these nanoclays should exhibited less viscosity decrease. This is true for the addition of D43B and the better dispersion of this nanoclays in the PLA matrix observed in SEM (Figure 4.5) results could contribute to this higher thermal stability achieved. The presence of aggregates in nanocomposites containing C15A and the minor d-spacing of interlayers achieved could explain the higher intrinsic viscosity decrease.

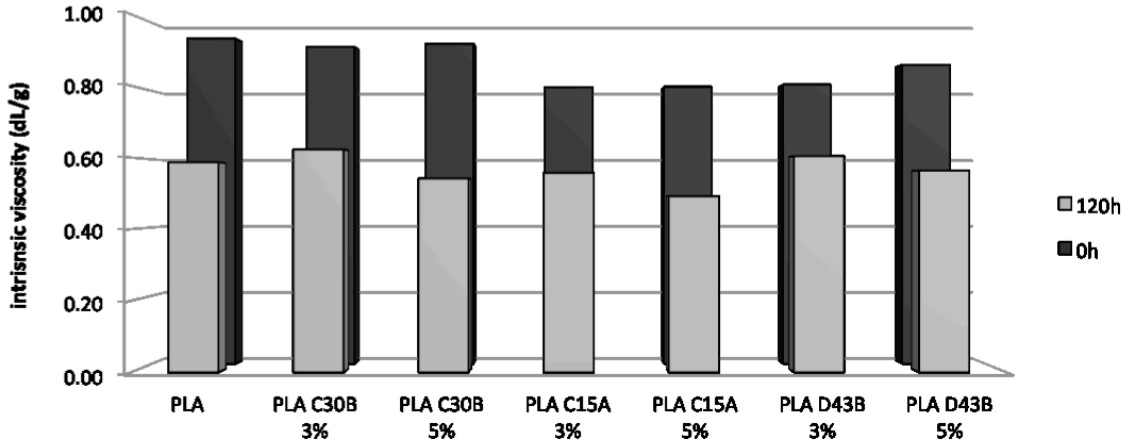

Figure 4.9 - Intrinsic viscosity (η) for initial and degraded samples.

4.2.3. FTIR analysis

FTIR spectra of PLA and PLA nanocomposites with 3 wt.% nanoclay incorporation obtained before and after 24, 96 and 120 hours of thermo-oxidative degradation are presented in Figures 4.10 to 4.13, respectively.

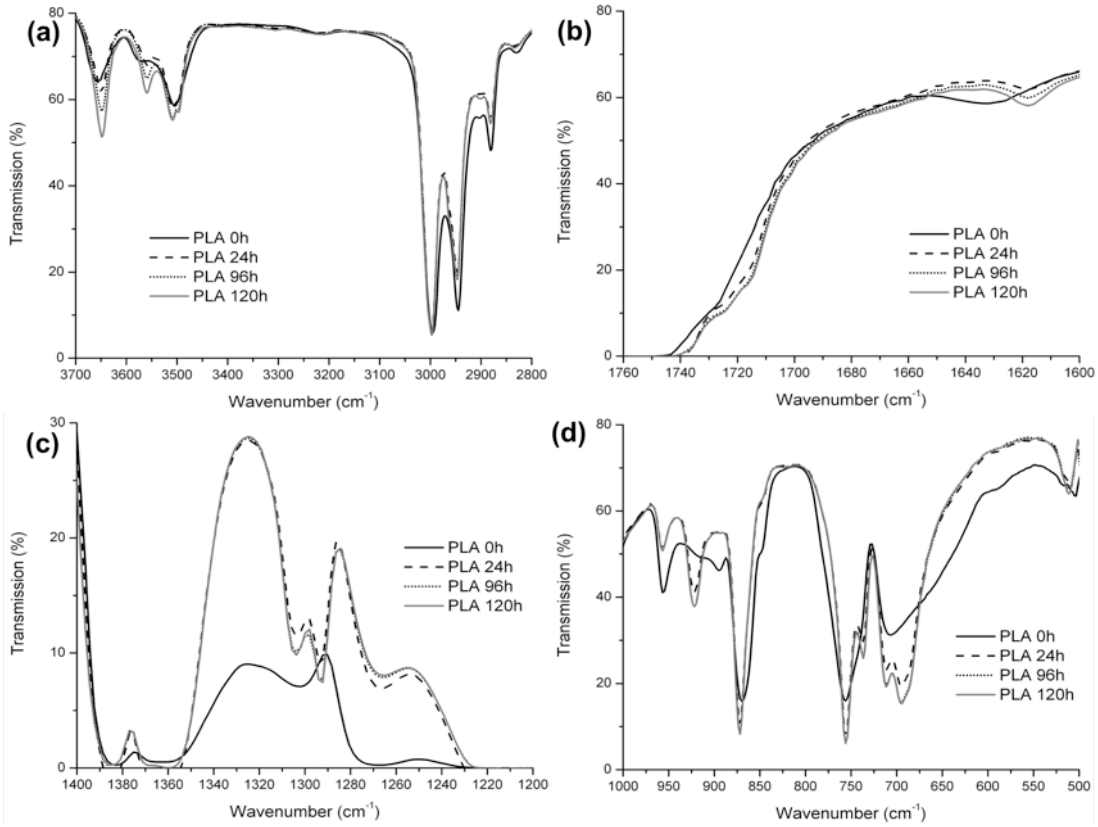

Figure 4.10 – FTIR spectra of PLA obtained before and after 24, 96 and 120 hours of thermo-oxidative degradation in four regions: a) 3700-2800 cm^{-1}, b) 1700-1600 cm^{-1}, c) 1400-1200 cm^{-1} and d) 1000-500 cm^{-1}.

In Figure 4.10 a) an increase of the bands in the 3650-3500 cm^{-1} region, assigned to OH end groups [88, 119] and free hydroxyl groups [121], was observed along degradation time, as well as a decrease in the bands 3000-2800 cm^{-1} attributed to CH deformation (including symmetric and asymmetric bands) [115, 116, 121].

A large and saturated band around 1750 cm^{-1} can be assigned to C=O from ester groups [115, 121] and Figure 4.10 b) shows two new shoulders at 1724 and 1714 cm^{-1} after degradation. These can be associated to the formation of new carbonyl compounds and, in the literature, the band at 1714 cm^{-1} was assigned to COOH [115].

A huge reduction in the band around 1380-1310 cm^{-1} attributed to CH linkages [115, 116, 121] (Figure 4.10 c) can be detected after degradation, which is in agreement with what was observed in Figure 4.10 a). Crystallization leads to a decrease of the band at 1267 cm^{-1} [118] assigned to CO stretch [115, 116, 121].

In the region from 1000 to 500 cm^{-1} showed in Figure 4.10 d) it can be seen a decrease of the amorphous band at 955 cm^{-1} [118] assigned to CH_3 and CC linkages [115, 116] and the appearance of a new band at 920 cm^{-1}, characteristic of α crystals. It is already known that the band at 869 cm^{-1} is assigned to the amorphous phase and the

band at 755 cm^{-1} to the crystalline phase [88, 115], and along degradation a small increase of both bands, C-COO and C=O vibrations, were observed [88, 115, 116, 121]. An increase and unfolding of the band around 700 cm^{-1}, which corresponds to C=O [116] was also detected.

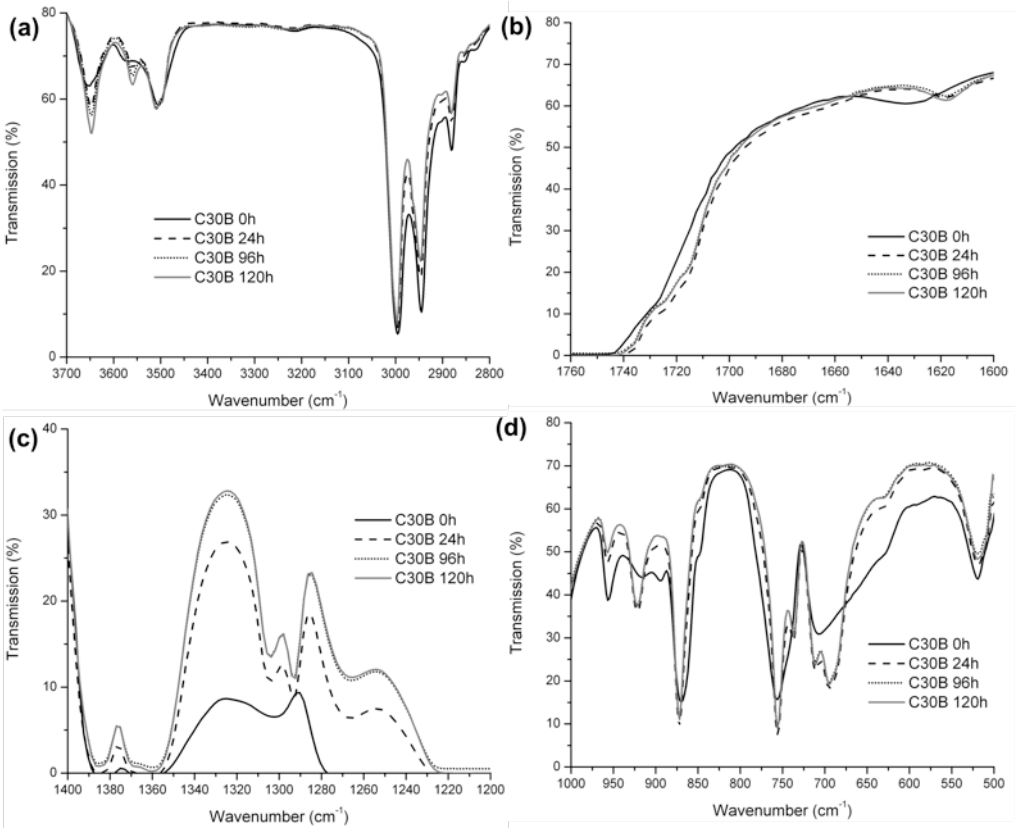

Figure 4.11 - FTIR spectra of PLA with 3 wt.% C30B obtained before and after 24, 96 and 120 hours of thermo-oxidative degradation in four regions: a) 3700-2800 cm^{-1}, b) 1700-1600 cm^{-1}, c) 1400-1200 cm^{-1} and d) 1000-500 cm^{-1}.

FTIR spectra obtained for PLA with 3 wt.% C30B are depicted in Figure 4.11. The overall FTIR spectrum is quite similar to the one obtained for PLA (Figure 4.10), no vibration modes are totally suppressed and no new modes seem to appear due to nanoclay presence. PLA structure changes are due to degradation and not due to nanoclay addiction. The results obtained with different nanoclays were similar (Figure 4.12 and 4.13).

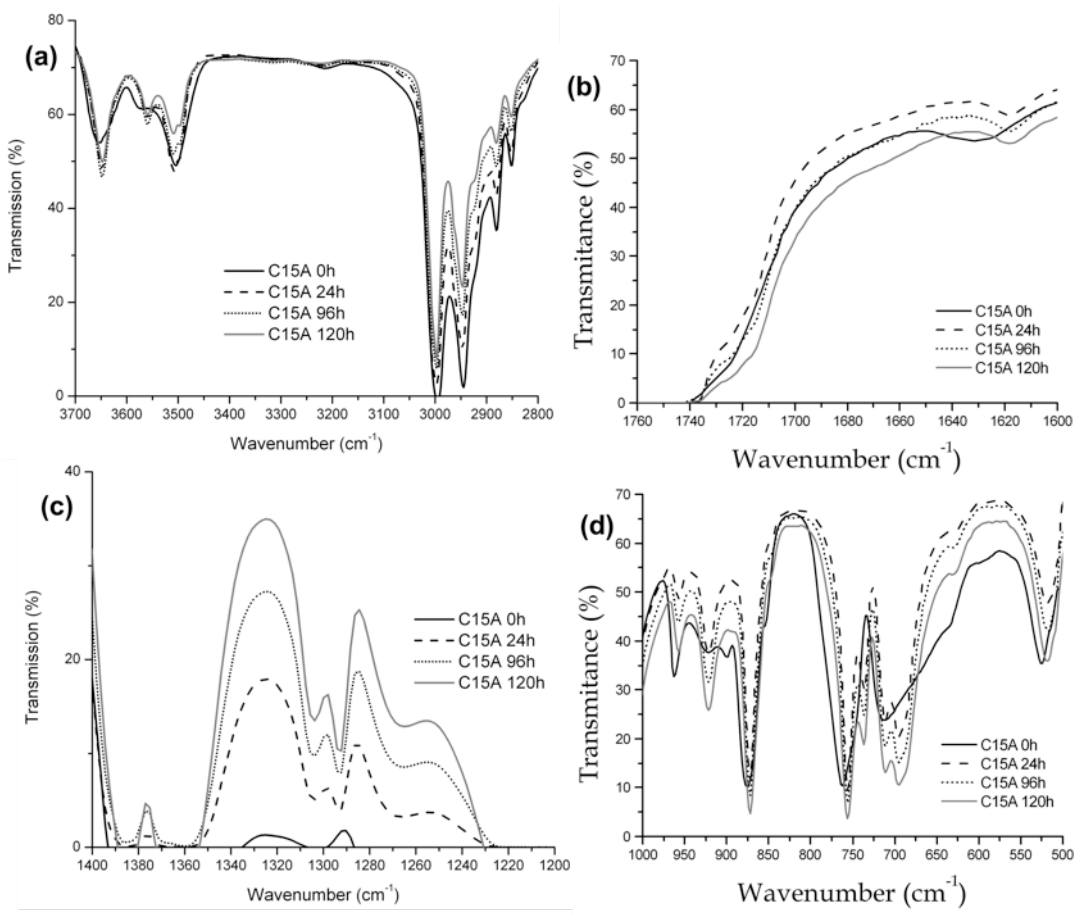

Figure 4.12 - FTIR spectra of PLA with 3 wt.% C15A obtained before and after 24, 96 and 120 hours of thermo-oxidative degradation in four regions: a) 3700-2800 cm^{-1}, b) 1700-1600 cm^{-1}, c) 1400-1200 cm^{-1} and d) 1000-500 cm^{-1}.

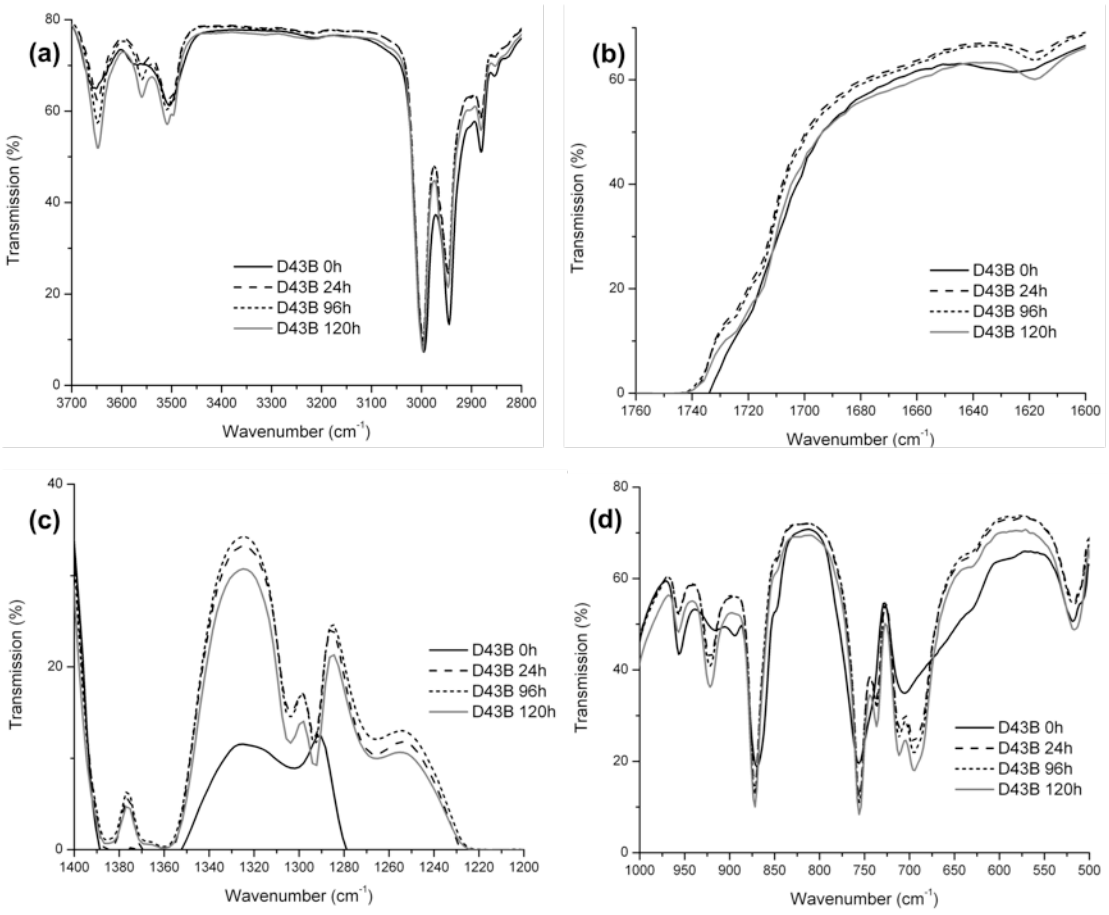

Figure 4.13 - FTIR spectra of PLA with 3 wt.% D43B obtained before and after 24, 96 and 120 hours of thermo-oxidative degradation in four regions: a) 3700-2800 cm^{-1}, b) 1700-1600 cm^{-1}, c) 1400-1200 cm^{-1} and d) 1000-500 cm^{-1}.

4.2.4. Thermal analysis

Thermal properties of PLA and PLA nanocomposites were evaluated by DSC. Figure 4.14 presents the crystallinity degree of PLA and PLA nanocomposites with 3 wt.% nanoclay before and after 120 hours of thermo-oxidative degradation.

It is known that the addition of the nanoclays promotes the extent of crystallization of PLA during heating indicating that they can act as nucleating agents [64, 130]. This was observed for C30B and D43B probably due to the good dispersion achieved and to the lower molecular weight observed before. With the incorporation of C15A a non-expected decrease in crystallinity degree was observed probably due to the heterogeneity and aggregates formation observed in this sample.

After 120 hours of thermo-oxidative degradation an increase of the crystallinity degree can be observed for all samples. This increase was higher for nanocomposites. This increase is due to the hydrolysis of the PLA chains, in the amorphous region rather than in the crystalline because they are more accessible. The shorter PLA chains have higher mobility and they can reorganize easily, which leads to an increase of

crystallinity degree [121, 129]. As expected, due to the higher chain scission induced by hydroxyl groups, the nanocomposites with C30B presents higher crystallinity degree after degradation.

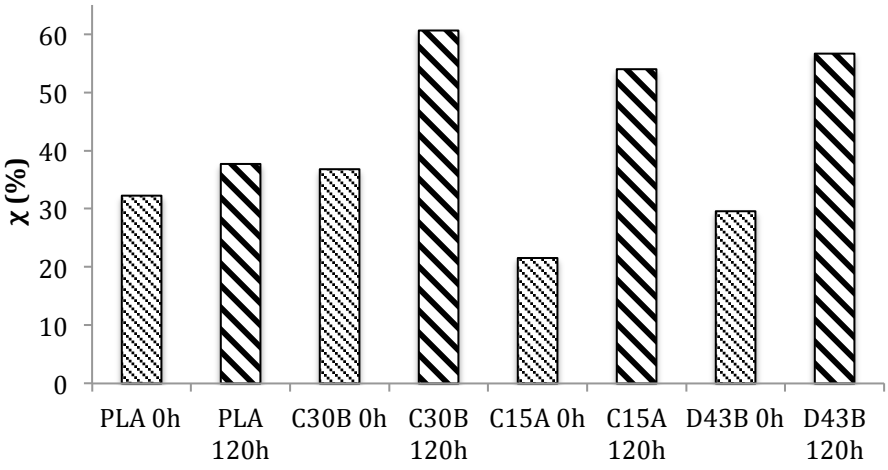

Figure 4.14 - Crystallinity degree (χ) of initial and degraded samples with 3 wt.% nanoclay incorporation.

Table 4.4 presents T_g and T_m values obtained from DSC analysis. It can be firstly noted that the PLA T_g in the nanocomposites appears to de slightly higher than PLA. This behaviour has been observed by other authors [45, 69] and is ascribed to the restricted segmental motions at the organic–inorganic interface neighbourhood of intercalated compositions. The nanoclay incorporation does not affect the T_m of the nanocomposites in agreement with what was observed by other authors [84, 89].

Table 4.4 – T_m and T_g values obtained for PLA and PLA nanocomposites with 3 wt.% nanoclays incorporation.

Samples	T_g (°C)	T_m (°C)
PLA 0h	48.5	164.5
PLA 120h	-	164.5
PLA/C30B 0h	57.3	166.6
PLA/C30B 120h	-	164.8
PLA/C15A 0h	50.7	164.9
PLA/C15A 120h	-	164.6
PLA/D43B 0h	50.3	164.5
PLA/D43B 120h	-	164.7

4.3. Photo-oxidative degradation

In order to obtain information about UV stability of PLA and PLA nanocomposites, initial samples were submitted to photo-oxidative degradation in an accelerated chamber as described in Experimental Chapter (3.3.2). The degraded samples were then analysed by NMR, FTIR, viscosimetry and DSC and the results compared with the ones obtained for initial materials.

4.3.1. ^{1}H NMR analysis

In order to evaluate if visible changes in the chemical structure of PLA were observed during photo-oxidative degradation, degraded samples were analysed by ^{1}H NMR. The δ values obtained in the ^{1}H NMR spectra and the corresponding groups are listed in Table 4.5. It can be observed that the assignments obtained are in well agreement with literature [115]. No changes in chemical shift values are observed between PLA 0 h, PLA 300 h and PLA 600 h. However, there are differences in the signal intensities and in proton area ratio (CH_3/CH), which decrease with degradation. This was already explained previously in NMR results from thermo-oxidative degraded samples.

Table 4.5 - ^{1}H NMR data for PLA samples.

	δ CH_3 (ppm)	δ CH (ppm)	Relative area CH_3/CH
PLA 0h	1.56 – 1.60	5.14 – 5.21	3.71
PLA 300h	1.58 – 1.60	5.14 – 5.21	3.26
PLA 600h	1.58 – 1.60	5.13 – 5.20	3.18

4.3.2. Intrinsic viscosity measurements

Intrinsic viscosity (η) measurements were performed in degraded samples along time together with the initial values (Figure 4.15). An initial decrease in η is observed for all nanocomposites. Reasons for these changes may involve the shear during melt mixing of PLA and nanoclay. Hydrolysis of the PLA matrix is accelerated by the high temperature, shear and the reactive groups of the modifiers of each clay [45, 121].

PLA η decrease slightly after 200 hours of photo-oxidative degradation and then this value remain practically unchanged until 600 hours. η of nanocomposites gradually decrease with increase of degradation time and the major decreases were observed with C30B and C15A. The reduction of the η of the PLA and PLA nanocomposites films indicates that chain scission plays an important role among the degradation

mechanisms. The photo-degradation of PLA is reported to cause chain cleavage and the formation of lower molecular weight compounds [44, 131].

As can be seen in Figure 4.15, the absolute slope of the lines adjusted to the experimental values, is an indicator of photo-oxidative degradation rate, is higher in nanocomposites with C30B and C15A. The presence of hydroxyl groups in C30B associated to good nanoclay dispersion and an intercalated structure may accelerate the photo-oxidative degradation of PLA and the formation of lower molecular weight compounds. As C15A did not present reactive functional groups, the high decrease in η may be explained by the presence of aggregates in PLA matrix.

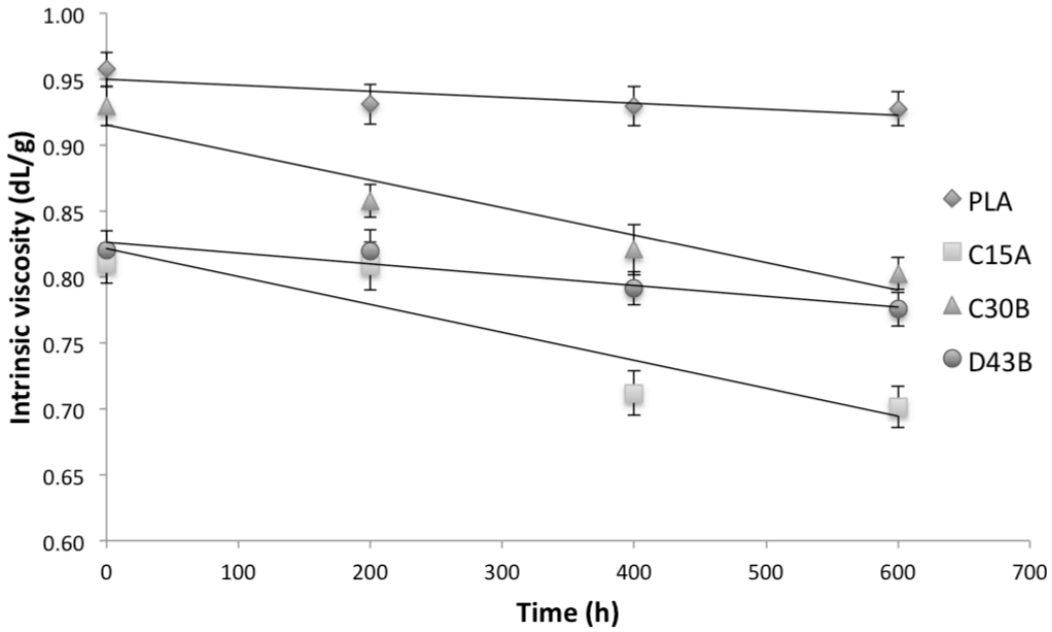

Figure 4.15 - Intrinsic viscosity of initial and along degradation samples of PLA and PLA nanocomposites.

4.3.3. FTIR analysis

FTIR spectra of PLA and PLA nanocomposites with 3 wt.% nanoclay addiction, recorded in three different regions, were obtained before and after 300 and 600 hours of photo-oxidative degradation.

The infrared spectra of PLA during photo-oxidative degradation (Figure 4.16) present the characteristic bands of the polymer [88, 115, 116, 118, 119, 121]. No significant changes are observed in the chemical structure of PLA after degradation: no vibration modes are suppressed; no new modes seem to appear due to degradation time and only slight increase intensity in some bands are observed. This is in concordance with viscosity measurements, as photo-degraded PLA did not show significant decrease of intrinsic viscosity.

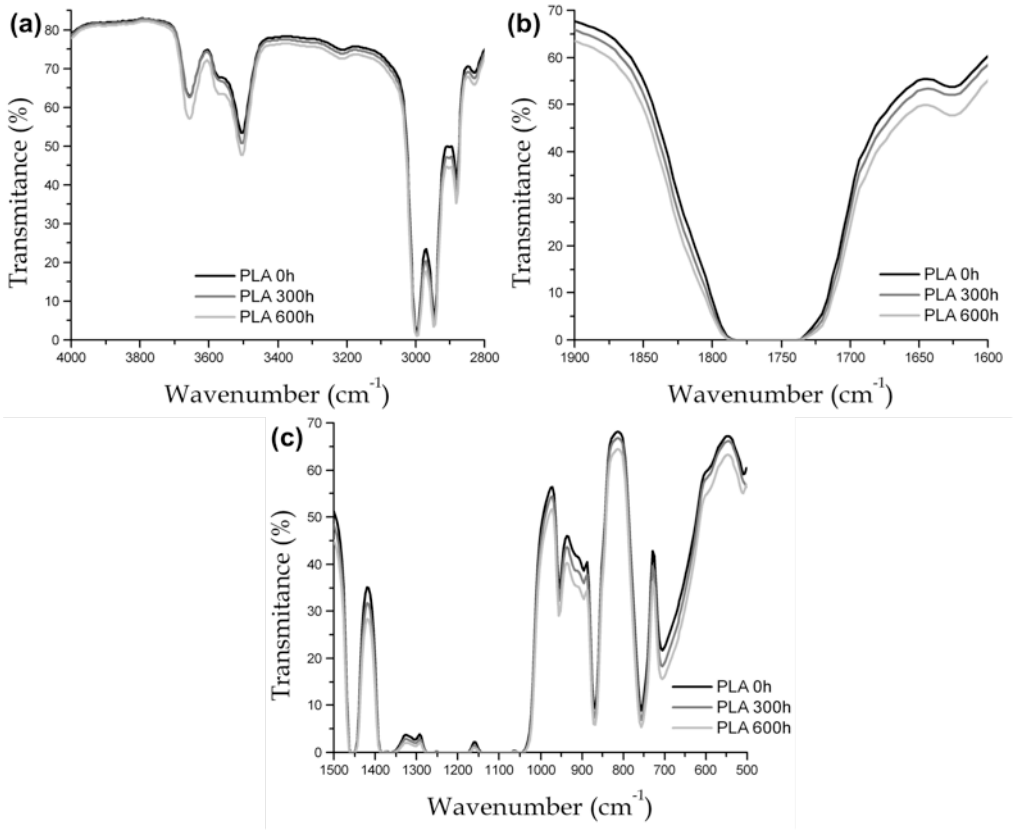

Figure 4.16 - FTIR spectra of PLA obtained before and after 300 and 600 hours of photo-oxidative degradation in three regions: a) 4000-2800 cm^{-1}, b) 1900-1600 cm^{-1} and c) 1500-500 cm^{-1}.

The photo-degradation of PLA was previously described in literature to occur according to a Norrish II mechanism (Figure 4.17) of carbonyl polyester [44, 55, 56]. This mechanism causes chain cleavage and the formation of C=C double bands and hydroperoxide O-H at newly formed chain terminals. However, this mechanism was proposed based on results obtained with a light source emitting in the UV domain from 220 nm [55], thus, in a region where the carbonyl groups of aliphatic polyester can absorb energy an consequently lead to photoreaction [120, 122]. These conditions do not simulate natural outdoor exposure, so in this work the UV light wavelengths bellow 300 nm were filtered (Figure 3.3).

Based on the formation of anhydride, new mechanisms for PLA photo-degradation have been proposed [120, 122, 132]. Figure 4.18 presents PLA photo-degradation mechanism proposed by Bocchini et al. [122]. Photo-degradation usually begins by radical formed from impurities by UV-irradiation or thermal decomposition. The reaction with higher probability is the abstraction of tertiary hydrogen from PLA chain with the formation of a tertiary radical P• (1). This radical can react with oxygen to form a peroxide radical (2), which may easily abstract another hydrogen from a tertiary

carbon with the formation of an hydroperoxide and the initial radical P• (3). Then, the hydroperoxide undergoes photolysis (4) with the formation of the HO• and a PO• radical that can further evolve by β-scission (5). Taking into account the stability of the different fragments the most probable β-scission appears to be the (5b) reaction, leading to the formation of anhydride groups.

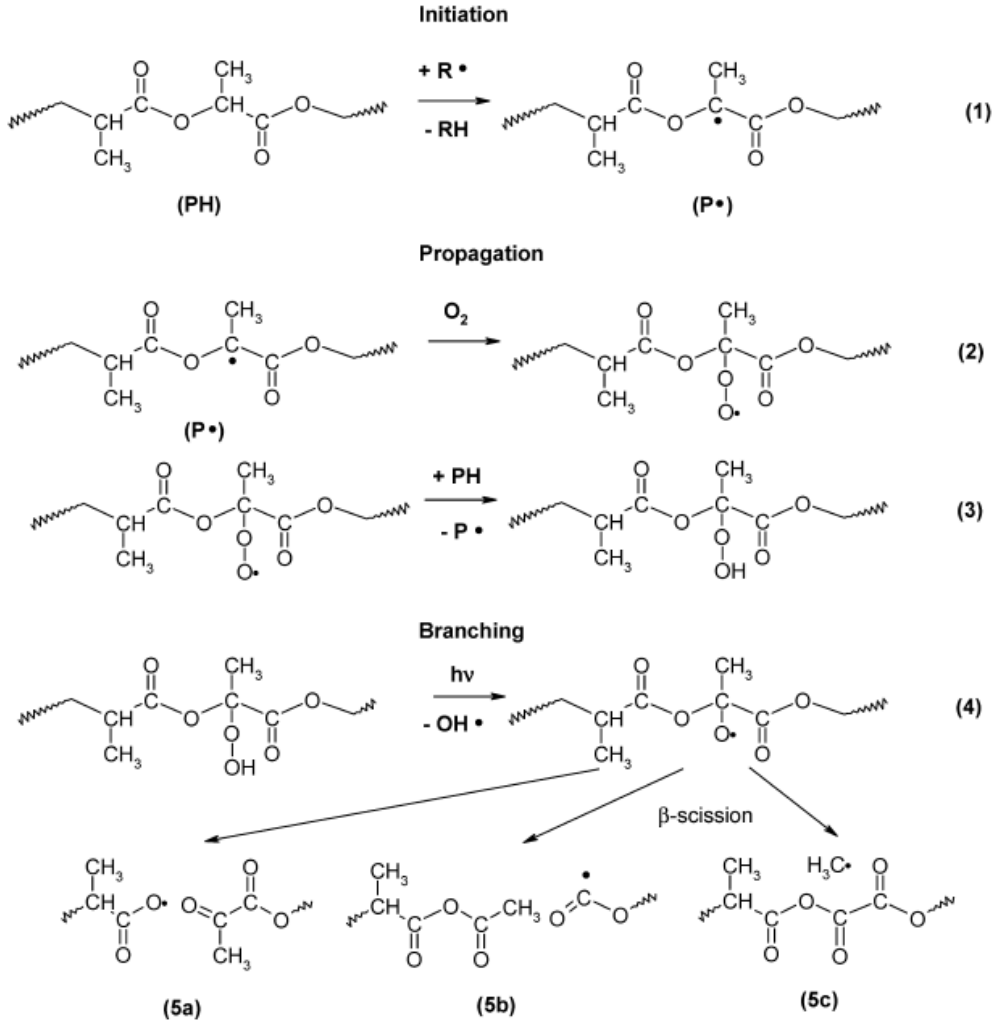

Figure 4.17 – PLA photo-degradation mechanism proposed by Bocchini et al. [122].

Janorkar et al. [132] reported the occurrence of two mechanisms for the degradation of PLA under UV irradiation. As described in Figure 4.17, the first mechanism involves a photolysis reaction leading to breakage of the backbone C–O bond. The second one involves photo-oxidation of PLA leading to the formation of hydroperoxide and its subsequent degradation to compounds containing a carboxylic acid and diketone end groups. Furthermore, the photolysis of the diketone may lead to the homolytic cleavage of the C–O bond between the two carbonyl groups, resulting in two carbonyl radicals. This radical pair can undergo cage escape to form several photo products.

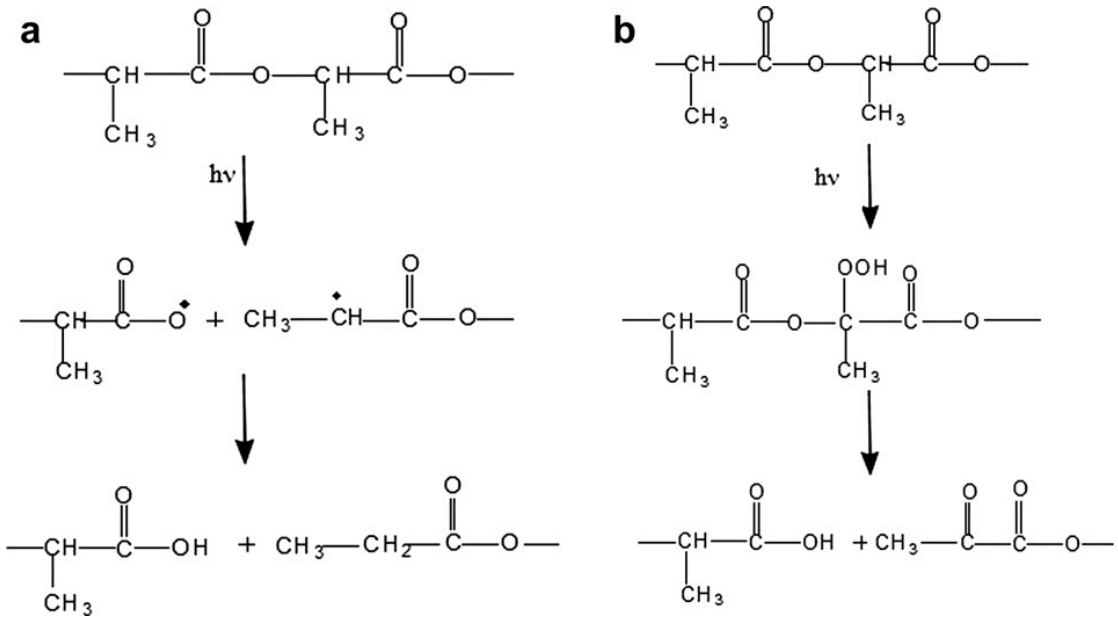

Figure 4.18 – a) and b) represent two PLA photo-degradation mechanisms proposed by Janorkar et al. [132].

Gardette et al. [120] propose the mechanism shown in Figure 4.19. This mechanism involves a classical hydrogen abstraction on the polymeric backbone at the tertiary carbon in the α-position of the ester function leading to the formation of macroradicals. It is postulated that initiation of the photochemical reaction results from the presence of chromophoric defects in the polymer at very low concentrations.

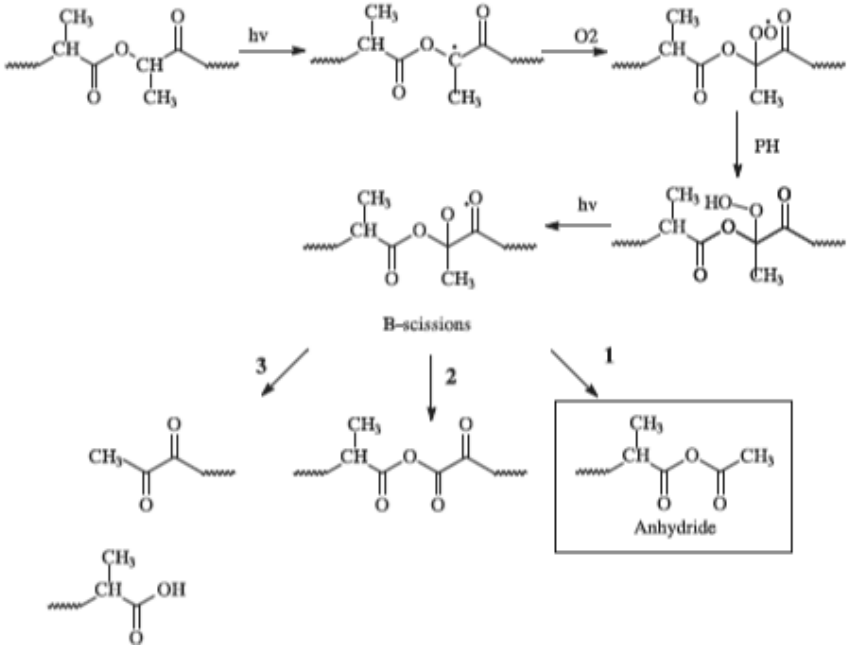

Figure 4.19 - PLA photo-degradation mechanism proposed by Gardette et al. [120].

Figure 4.20 shows the characteristic infrared spectra obtained for PLA/C30B. The overall response of the FTIR spectra is quite similar to the one obtained for PLA (Figure 4.16) therefore, any changes on PLA structure are due to degradation and not due to nanoclay addiction (the photo-degradation mechanism of PLA did not change with nanoclay addiction). It is observed higher band intensity for the nanocomposites compared to the polymer after degradation, enlargement of the band corresponding to C=O and the appearance and increase with degradation time of a shoulder at 1845 cm^{-1}. On the basis of the literature data, this band is assigned to anhydride groups [120, 122] and are in agreement with the photo-degradation mechanism proposed by Bocchini et al. [122] and Gardette et al. [120].

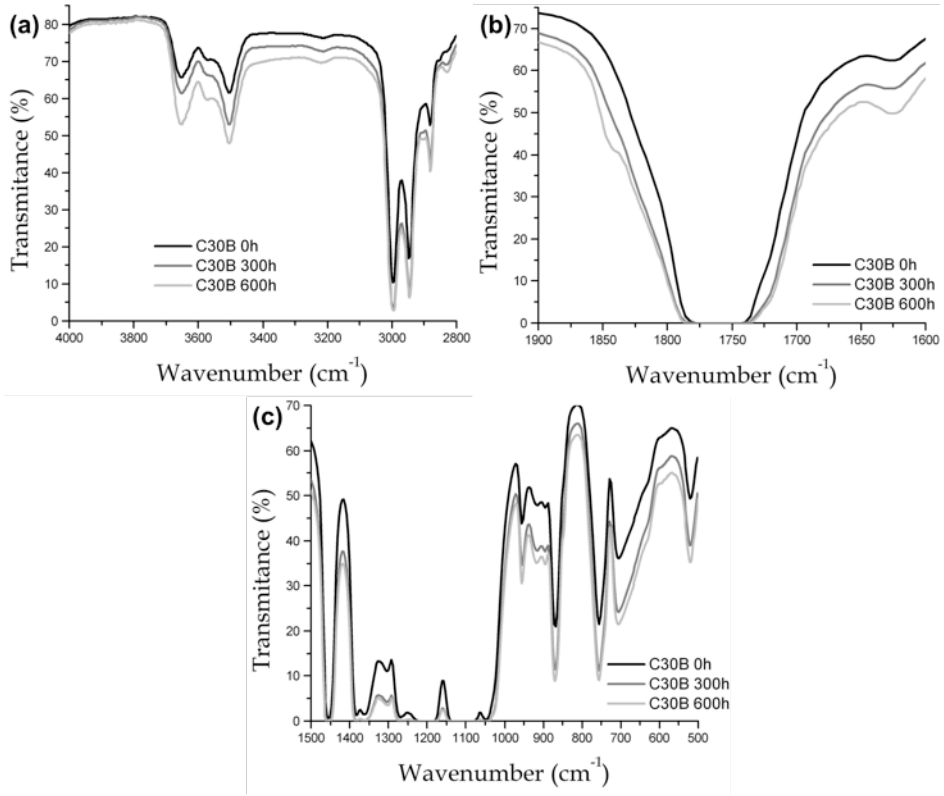

Figure 4.20 - FTIR spectra of PLA with 3 wt.% C30B obtained before and after 300 and 600 hours of photo-oxidative degradation in three regions: a) 4000-2800 cm^{-1}, b) 1900-1600 cm^{-1} and c) 1500-500 cm^{-1}.

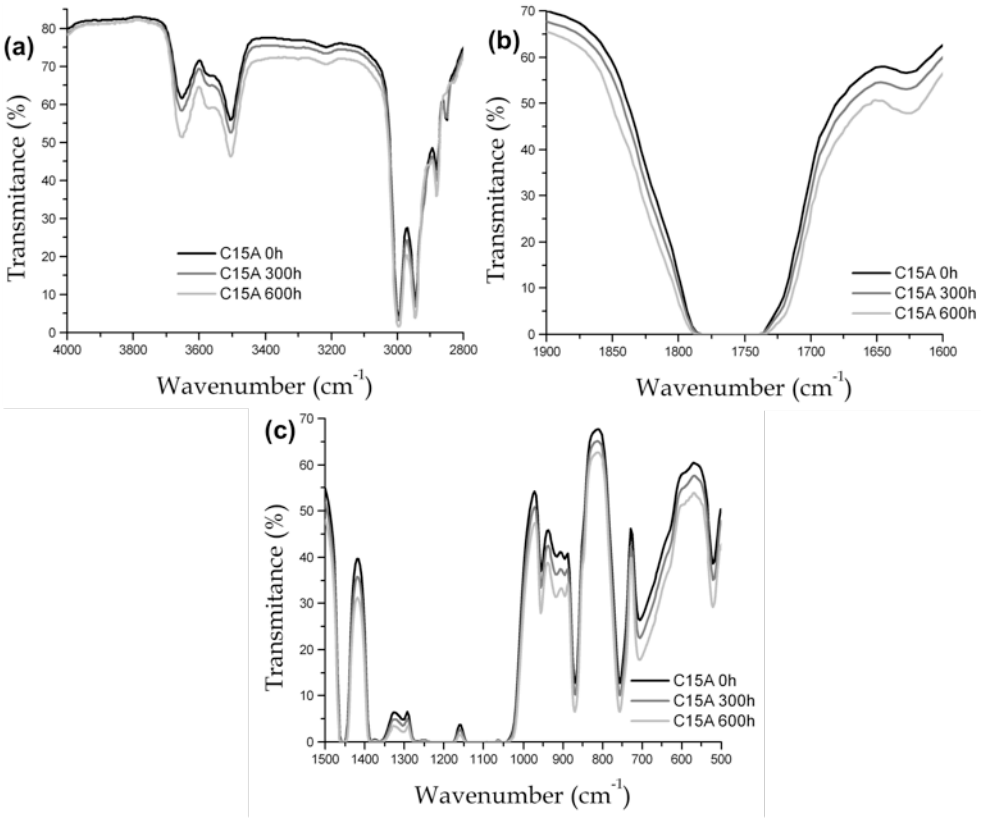

Figure 4.21 - FTIR spectra of PLA with 3 wt.% C15A obtained before and after 300 and 600 hours of photo-oxidative degradation in three regions: a) 4000-2800 cm^{-1}, b) 1900-1600 cm^{-1} and c) 1500-500 cm^{-1}.

Results obtained with C15A (Figure 4.21) and D43B (Figure 4.22) incorporation were similar to the one with C30B, without the appearance of the band at 1845 cm^{-1}.

These results show that nanoclay incorporation seems to enhance PLA photo-oxidative degradation, specially C30B.

According to the literature [58, 88, 115, 118], there are bands related to amorphous phase of PLA (955 and 869 cm^{-1}) and to crystalline phase (755, 912 and 923 cm^{-1}). As all these bands are present in FTIR spectra of the PLA and PLA nanocomposites and all of them increase with degradation time, the results were not elucidative in what concerns to the effect of photo-oxidative degradation on crystallinity. In order to overcome this problem, DSC measurements were performed.

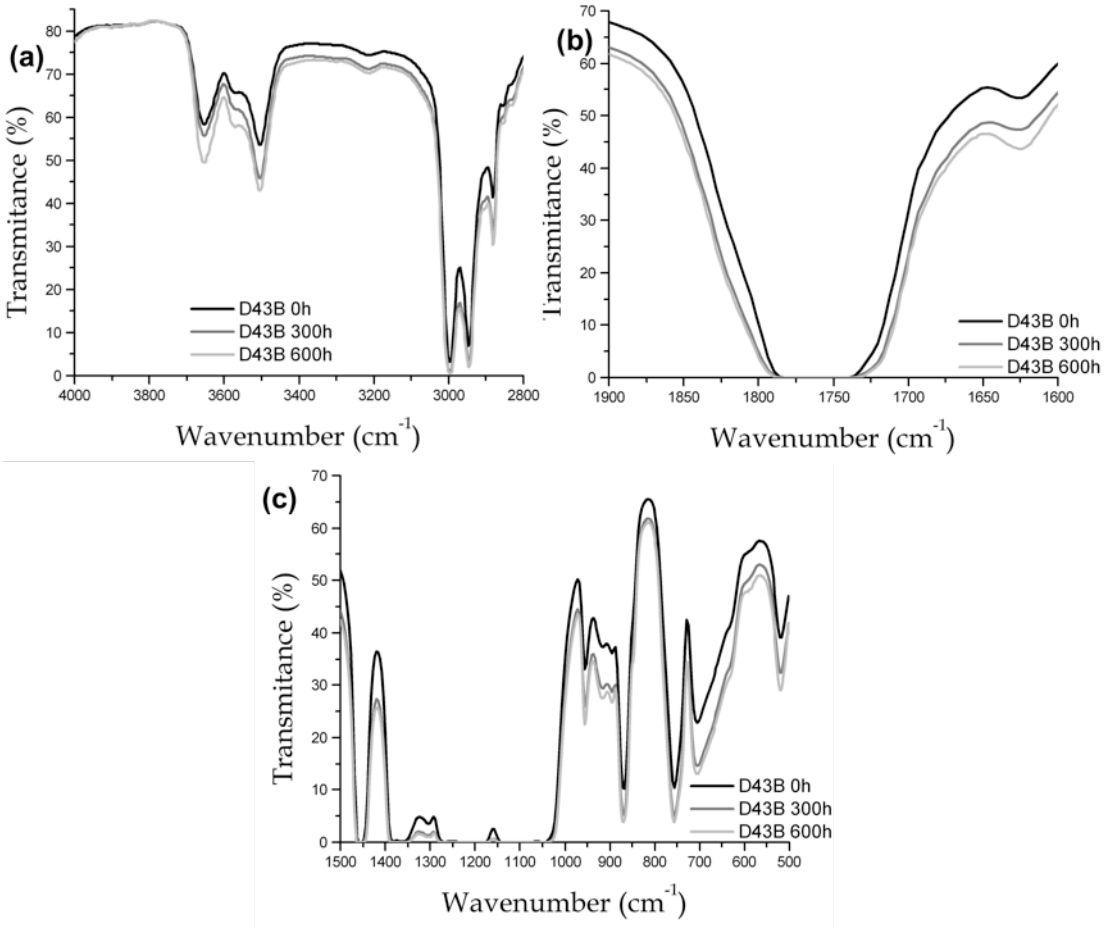

Figure 4.22 - FTIR spectra of PLA with 3 wt.% D43B obtained before and after 300 and 600 hours of photo-oxidative degradation in three regions: a) 4000-2800 cm^{-1}, b) 1900-1600 cm^{-1} and c) 1500-500 cm^{-1}.

4.3.4. Thermal analysis

Thermal properties of PLA and PLA nanocomposites were evaluated by DSC and Figure 4.23 show the DSC curves of photo-degraded samples after 600 h. The results show that photo-oxidative degradation does not affect the T_m of the PLA and PLA nanocomposites.

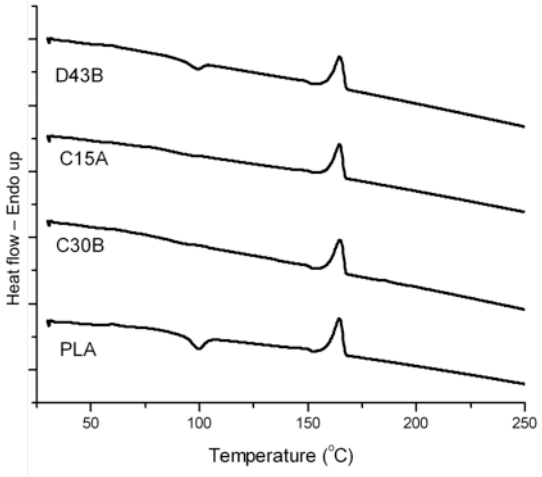

Figure 4.23 – DSC curves of PLA and PLA nanocomposites photo-degraded after 600 hours.

Figure 4.24 presents the crystallinity degree of PLA and PLA nanocomposites before and after 600 hours of photo-oxidative degradation.

It is known that the addition of the nanoclays promotes the extent of crystallization of PLA on heating indicating that they can act as nucleating agents [64, 130]. This was observed for initial nanocomposites with C30B and D43B but not for PLA/C15A as the χ was minor than for initial PLA.

With degradation an increase of χ is observed for all samples, specially for nanocomposites. This is in concordance with viscosity and infrared resusts as the higher differences were found on nanocomposites samples. This results indicate that the addiction of nanoclays can promote PLA photo-oxidative degradation.

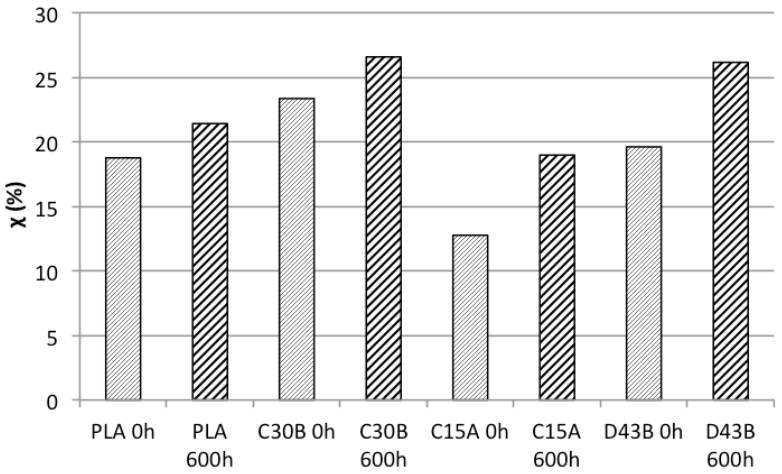

Figure 4.24 - Crystallinity degree (χ) of initial and 600 hours degraded samples.

Chapter 5

Conclusions

"We know very little, and yet it is astonishing that we know so much, and still more astonishing that so little knowledge can give us so much power."

— Bertrand Russell

This work is original and contributes to increase the scientific knowledge. Until now no work was published concerning PLA thermo-oxidative degradation in an oven with different type and amount of nanoclays (most of these studies used TGA) and only two works have been devoted to the study of PLA nanocomposites UV stability. However, one of the works is related to natural weathering and the other uses other nanoclays.

The research presented in this thesis aimed to evaluate the influence of different nanoclays addiction (Cloisite 30B, Cloisite 15A and Dellite 43B) and different nanoclay amount (3 and 5 % in weight) on the thermal and UV stability of PLA. Therefore, this work began with the preparation of PLA and PLA nanocomposites by melt mixing and obtaining thin films in a hot press.

The prepared materials were characterized by XRD showing that nanoclays were intercalated in the PLA matrix. However, according to SEM results, better nanoclay dispersion were obtained for PLA nanocomposites with C30B and nanoclay aggregates were found in the case of C15A. Chemical structure analyses by FTIR and 1H-NMR show that no significant changes in PLA occurred as a result of nanoclays incorporation. As expected, PLA sensitivity to melt processing was observed by the decrease of intrinsic viscosity, mainly in the case of nanocomposites. According to TGA results, the addiction of nanoclays seems to enhance the thermal stability of PLA under non-oxidative atmosphere.

PLA and PLA nanocomposites were submitted to thermo-oxidative degradation and results from ^{1}H-NMR and intrinsic viscosity showed that chain scission occurred after 120 hours of degradation. Changes in FTIR spectra of degraded samples evidence the formation of new carbonyl compounds. With 3 wt.% nanoclays incorporation, less difference between initial and degraded samples intrinsic viscosity was observed, indicating that the addition of this amount of nanoclays could enhance the PLA thermal stability under oxidative conditions. The addition of D43B seemed to contribute to increase PLA thermal stability since the intrinsic viscosity differences between initial and degraded samples were minor.

The reduction of the intrinsic viscosity of the PLA and PLA nanocomposites films, along 600 hours in an accelerated chamber, indicates that chain scission plays an important role among the degradation mechanisms and photo-oxidative degradation rates were higher for nanocomposites C30B and C15A. FTIR spectra of PLA did not present significant changes along degradation. However, in nanocomposites a shoulder at 1845 cm^{-1} appeared and increased with degradation time, which indicate that the presence of nanoclays enhanced photo-oxidative degradation according to a proposed

mechanism that leads to anhydride formation. DSC results evidence that nanoclays had a nucleation effect on PLA and lower molecular weight compounds were formed as the crystallinity degree of samples increase with degradation.

PLA nanocomposites prepared in the present work exhibited higher thermal stability and lower photo stability than PLA.

Chapter 6

Future perspectives

"I do not know what I may appear to the world, but to myself I seem to have been only like a boy playing on the sea-shore, and diverting myself in now and then finding a smoother pebble or a prettier shell than ordinary, whilst the great ocean of truth lay all undiscovered before me."

— Isaac Newton

Nowadays, high quantities of plastic materials, usually discarded after the first use, lead to a negative impact on the environment. To overcome this problem the interest on biodegradable polymers, like PLA, increased. However, the development of PLA materials for wide applications needs information about thermal and UV stability.

Take into consideration the results and conclusions of the present research, some future work can be recommended.

- A more detailed investigation of the nanocomposites preparation is required to explore and obtain exfoliated structures and analysis with TEM can also give important information;

- For industrial applications, the evaluation of the nanocomposites mechanical properties is very important;

- One of the most promising directions of this research would be further investigation of PLA nanocomposites biodegradation;

- It would be also very interesting to continue the degradation studies with more nanoclays type and amount;

- Given the importance of PLA use in food packaging applications, permeability experiments to oxygen should be carried out.

Chapter 7

References

"Never memorize something that you can look up."

— Albert Einstein

[1] Harper, C.A., *Handbook of plastics technologies : the complete guide to properties and performance*. **2006**, McGraw-Hill, New York.

[2] Morton-Jones, D.H., *Polymer processing*. **1989**, Chapman and Hall, London; New York.

[3] Nicholson, J.W. and Royal Society of, C., *The chemistry of polymers*. **1991**, Royal Society of Chemistry, Cambridge [England].

[4] Young, R.J. and Lovell, P.A., *Introduction to polymers*. **1991**, Chapman & Hall, London.

[5] Kumar, A. and Gupta, R.K., *Fundamentals of polymer engineering*. **2003**, Marcel Dekker, New York.

[6] Gnanou, Y., Fontanille, M. and Fontanille, M., *Organic and physical chemistry of polymers*. **2008**, Wiley-Interscience, Hoboken, N.J.

[7] Callister, W.D., *Materials science and engineering : an introduction*. **2006**, John Wiley & Sons, Hoboken, NJ.

[8] Bower, D.I., *An introduction to polymer physics*. **2002**, Cambridge University Press, Cambridge; New York.

[9] Morawetz, H., *Polymers : the origins and growth of a science*. **2002**, Dover Publications, New York.

[10] Pearce, E.M., *Polymers*. **1995**, National Academy Press, Washington, D.C.

[11] Zhang, M.Q. and Rong, M.Z., *Self-healing polymers and polymer composites*. **2011**, Wiley, Hoboken, N.J.

[12] Hunt, B.J. and James, M.I., *Polymer characterisation*. **1993**, Blackie Academic & Professional, London; New York.

[13] Ryan, A.J., *Emerging themes in polymer science*. **2001**, Royal Society of Chemistry, Cambridge.

[14] Gupta, R.K., Kennel, E. and Kim, K.-J., *Polymer nanocomposites handbook*. **2010**, CRC Press, Boca Raton.

[15] Paul, D. and Robeson, L., *Polymer nanotechnology: nanocomposites*. Polymer, **2008**, 49(15) 3187-3204.

[16] Lagaron, J.M. and Lopez-Rubio, A., *Nanotechnology for bioplastics: opportunities, challenges and strategies*. Trends in Food Science & Technology, **2011**, 22(11) 611-617.

[17] Bhattacharya, S.N., Kamal, M.R. and Gupta, R.K., *Polymeric nanocomposites theory and practice*. **2008**, Carl Hanser Publishers ; Hanser Gardner Publications, Munich; Cincinnati, Ohio.

[18] Leng, J. and Lau, A.K.T., *Multifunctional polymer nanocomposites*. **2011**, CRC Press, Boca Raton.

[19] Ajayan, P.M., Schadler, L.S. and Braun, P.V., *Nanocomposite science and technology*. **2003**, Wiley-VCH, Weinheim.

[20] Thomas, S. and Zaikov, G.E., *Polymer nanocomposite research advances*. **2008**, Nova Science Publishers, New York.

[21] Żenkiewicz, M. and Richert, J., *Permeability of polylactide nanocomposite films for water vapour, oxygen and carbon dioxide*. Polymer Testing, **2008**, 27(7) 835-840.

[22] Picard, E., Espuche, E. and Fulchiron, R., *Effect of an organo-modified montmorillonite on PLA crystallization and gas barrier properties*. Applied Clay Science, **2011**, 53(1) 58-65.

[23] Hua, L., Kai, W., Yang, J.*, et al.*, *A new poly(l-lactide)-grafted graphite oxide composite: Facile synthesis, electrical properties and crystallization behaviors*. Polymer Degradation and Stability, **2010**, 95(12) 2619-2627.

[24] Vilaplana, F., Strömberg, E. and Karlsson, S., *Environmental and resource aspects of sustainable biocomposites*. Polymer Degradation and Stability, **2010**, 95(11) 2147-2161.

[25] Fukushima, K., Tabuani, D. and Camino, G., *Nanocomposites of PLA and PCL based on montmorillonite and sepiolite*. Materials Science and Engineering: C, **2009**, 29(4) 1433-1441.

[26] Madhavan Nampoothiri, K., Nair, N.R. and John, R.P., *An overview of the recent developments in polylactide (PLA) research*. Bioresour Technol, **2010**, 101(22) 8493-501.

[27] Amass, W., Amass, A. and Tighe, B., *A review of biodegradable polymers: uses, current developments in the synthesis and characterization of biodegradable polyesters, blends of biodegradable polymers and recent advances in biodegradation studies*. Polymer International, **1998**, 47(2) 89-144.

[28] Badía, J.D., Strömberg, E., Ribes-Greus, A.*, et al.*, *Assessing the MALDI-TOF MS sample preparation procedure to analyze the influence of thermo-oxidative ageing and thermo-mechanical degradation on poly (Lactide)*. European Polymer Journal, **2011**, 47(7) 1416-1428.

[29] Sinha Ray, S., Yamada, K., Okamoto, M.*, et al.*, *New polylactide-layered silicate nanocomposites. 2. Concurrent improvements of material properties, biodegradability and melt rheology*. Polymer, **2003**, 44(3) 857-866.

[30] Sinharay, S. and Bousmina, M., *Biodegradable polymers and their layered silicate nanocomposites: In greening the 21st century materials world*. Progress in Materials Science, **2005**, 50(8) 962-1079.

[31] Dashora, K., Sisodiya, D. and Pandey, P., *Studies on biodegradable polymers: A brief review*. Journal of Pharmacy Research, **2012**, 5(2) 852-858.

[32] Bordes, P., Pollet, E. and Averous, L., *Nano-biocomposites: Biodegradable polyester/nanoclay systems*. Progress in Polymer Science, **2009**, 34(2) 125-155.

[33] Hoidy, W.H., Al-Mulla, E.A.J. and Al-Janabi, K.W., *Mechanical and Thermal Properties of PLLA/PCL Modified Clay Nanocomposites*. Journal of Polymers and the Environment, **2010**, 18(4) 608-616.

[34] Kolybaba, M., Tabil, L., Panigrahi, S.*, et al.*, *Biodegradable polymers: past, present, and future*. **2003**, An ASAE Meeting Presentation,

[35] Avérous, L., *Biodegradable multiphase systems based on plasticized starch: a review*. Journal of Macromolecular Science, Part C: Polymer Reviews, **2004**, 44(3) 231-274.

[36] Luiz de Paula, E., Mano, V. and Pereira, F.V., *Influence of cellulose nanowhiskers on the hydrolytic degradation behavior of poly(d,l-lactide)*. Polymer Degradation and Stability, **2011**, 96(9) 1631-1638.

[37] Sarasua, J., Arraiza, A.L., Balerdi, P.*, et al.*, *Crystallization and thermal behaviour of optically pure polylactides and their blends*. Journal of materials science, **2005**, 40(8) 1855-1862.

[38] Rasal, R.M., Janorkar, A.V. and Hirt, D.E., *Poly (lactic acid) modifications*. Progress in Polymer Science, **2010**, 35(3) 338-356.

[39] Vink, E.T.H., Rabago, K.R., Glassner, D.A., *et al.*, *Applications of life cycle assessment to NatureWorks (TM) polylactide (PLA) production*. Polymer Degradation and Stability, **2003**, 80(3) 403-419.

[40] Cheng, Y., Deng, S., Chen, P., *et al.*, *Polylactic acid (PLA) synthesis and modifications: a review*. Frontiers of Chemistry in China, **2009**, 4(3) 259-264.

[41] Zhu, B., Li, J., He, Y., *et al.*, *Effect of steric hindrance on hydrogen-bonding interaction between polyesters and natural polyphenol catechin*. Journal of Applied Polymer Science, **2004**, 91(6) 3565-3573.

[42] Lim, L.T., Auras, R. and Rubino, M., *Processing technologies for poly(lactic acid)*. Progress in Polymer Science, **2008**, 33(8) 820-852.

[43] Tsuji, H., *Poly(lactide) stereocomplexes: formation, structure, properties, degradation, and applications*. Macromol Biosci, **2005**, 5(7) 569-97.

[44] Belbachir, S., Zaïri, F., Ayoub, G., *et al.*, *Modelling of photodegradation effect on elastic–viscoplastic behaviour of amorphous polylactic acid films*. Journal of the Mechanics and Physics of Solids, **2010**, 58(2) 241-255.

[45] Zhou, Q. and Xanthos, M., *Nanosize and microsize clay effects on the kinetics of the thermal degradation of polylactides*. Polymer Degradation and Stability, **2009**, 94(3) 327-338.

[46] Ito, M. and Nagai, K., *Degradation issues of polymer materials used in railway field*. Polymer Degradation and Stability, **2008**, 93(10) 1723-1735.

[47] Kim, K.J., Doi, Y. and Abe, H., *Effect of metal compounds on thermal degradation behavior of aliphatic poly(hydroxyalkanoic acid)s*. Polymer Degradation and Stability, **2008**, 93(4) 776-785.

[48] Nishida, H., Mori, T., Hoshihara, S., *et al.*, *Effect of tin on poly(l-lactic acid) pyrolysis*. Polymer Degradation and Stability, **2003**, 81(3) 515-523.

[49] Yuzay, I.E., Auras, R., Soto-Valdez, H., *et al.*, *Effects of synthetic and natural zeolites on morphology and thermal degradation of poly (lactic acid) composites*. Polymer Degradation and Stability, **2010**, 95(9) 1769-1777.

[50] Fan, Y., Nishida, H., Shirai, Y., *et al.*, *Thermal degradation behaviour of poly(lactic acid) stereocomplex*. Polymer Degradation and Stability, **2004**, 86(2) 197-208.

[51] Aoyagi, Y., Yamashita, K. and Doi, Y., *Thermal degradation of poly [-3-hydroxybutyrate], poly [ε-caprolactone], and poly [-lactide]*. Polymer Degradation and Stability, **2002**, 76(1) 53-59.

[52] McNeill, I. and Leiper, H., *Degradation studies of some polyesters and polycarbonates--2. Polylactide: Degradation under isothermal conditions, thermal degradation mechanism and photolysis of the polymer*. Polymer Degradation and Stability, **1985**, 11(4) 309-326.

[53] Singh, B. and Sharma, N., *Mechanistic implications of plastic degradation*. Polymer Degradation and Stability, **2008**, 93(3) 561-584.

[54] Jin, C., Christensen, P.A., Egerton, T.A., *et al.*, *Rapid measurement of polymer photo-degradation by FTIR spectrometry of evolved carbon dioxide*. Polymer Degradation and Stability, **2006**, 91(5) 1086-1096.

[55] Ikada, E., *Photo-and bio-degradable polyesters. Photodegradation behaviors of aliphatic polyesters*. Journal of Photopolymer Science and Technology, **1997**, 10(2) 265-270.

[56] Tsuji, H., Echizen, Y. and Nishimura, Y., *Enzymatic Degradation of Poly (l-Lactic Acid): Effects of UV Irradiation*. Journal of Polymers and the Environment, **2006**, 14(3) 239-248.

[57] Tsuji, H., Echizen, Y. and Nishimura, Y., *Photodegradation of biodegradable polyesters: A comprehensive study on poly (l-lactide) and poly (ε-caprolactone)*. Polymer Degradation and Stability, **2006**, 91(5) 1128-1137.

[58] Sato, S., Ono, M., Yamauchi, J.*, et al.*, *Effects of irradiation with vacuum ultraviolet xenon excimer lamp at 172nm on water vapor transport through poly (lactic acid) membranes*. Desalination, **2011**, 287(Special Issue) 290-300.

[59] Santos, R., Botelho, G. and Machado, A., *Artificial and natural weathering of ABS*. Journal of Applied Polymer Science, **2010**, 116(4) 2005-2014.

[60] Rabek, J.F., *Polymer photodegradation : mechanisms and experimental methods*. **1995**, Chapman & Hall, London.

[61] Gardette, J.L., Mailhot, B. and Lemaire, J., *Photooxidation mechanisms of styrenic polymers*. Polymer Degradation and Stability, **1995**, 48(3) 457-470.

[62] Mohd-Adnan, A.-F., Nishida, H. and Shirai, Y., *Evaluation of kinetics parameters for poly(l-lactic acid) hydrolysis under high-pressure steam*. Polymer Degradation and Stability, **2008**, 93(6) 1053-1058.

[63] Paul, M.A., Delcourt, C., Alexandre, M.*, et al.*, *Polylactide/montmorillonite nanocomposites: study of the hydrolytic degradation*. Polymer Degradation and Stability, **2005**, 87(3) 535-542.

[64] Fukushima, K., Tabuani, D., Dottori, M.*, et al.*, *Effect of temperature and nanoparticle type on hydrolytic degradation of poly(lactic acid) nanocomposites*. Polymer Degradation and Stability, **2011**, 96(12) 2120-2129.

[65] Lucas, N., Bienaime, C., Belloy, C.*, et al.*, *Polymer biodegradation: mechanisms and estimation techniques*. Chemosphere, **2008**, 73(4) 429-42.

[66] Auras, R., Harte, B. and Selke, S., *An overview of polylactides as packaging materials*. Macromol Biosci, **2004**, 4(9) 835-864.

[67] Pandey, J.K., Raghunatha Reddy, K., Pratheep Kumar, A.*, et al.*, *An overview on the degradability of polymer nanocomposites*. Polymer Degradation and Stability, **2005**, 88(2) 234-250.

[68] Choudalakis, G. and Gotsis, A.D., *Permeability of polymer/clay nanocomposites: A review*. European Polymer Journal, **2009**, 45(4) 967-984.

[69] Sinha Ray, S., Yamada, K., Okamoto, M.*, et al.*, *New polylactide/layered silicate nanocomposites. 5. Designing of materials with desired properties*. Polymer, **2003**, 44(21) 6633-6646.

[70] Bikiaris, D., *Can nanoparticles really enhance thermal stability of polymers? Part II: An overview on thermal decomposition of polycondensation polymers*. Thermochimica Acta, **2011**, 523(1-2) 25-45.

[71] Ublekov, F., Baldrian, J., Kratochvil, J.*, et al.*, *Influence of clay content on the melting behavior and crystal structure of nonisothermal crystallized poly (L-lactic acid)/nanocomposites*. Journal of Applied Polymer Science, **2012**, 124(2) 1643-1648.

[72] Weaver, C.E., *Clays, muds, and shales*. **1989**, Elsevier : Distributors for the U.S. and Canada, Elsevier Science Pub. Co., Amsterdam; New York.

[73] Meunier, A., *Clays*. **2005**, Springer, Berlin; New York.

[74] Duncan, T.V., *Applications of nanotechnology in food packaging and food safety: Barrier materials, antimicrobials and sensors*. Journal of colloid and interface science, **2011**, 363(1) 1-24.

[75] Kiliaris, P. and Papaspyrides, C.D., *Polymer/layered silicate (clay) nanocomposites: An overview of flame retardancy*. Progress in Polymer Science, **2010**, 35(7) 902-958.

[76] Marras, S.I. and Zuburtikudis, I., *Structure and thermal behavior of poly(L-lactic acid) clay nanocomposites: Effect of preparation method as a function of the nanofiller modification level*. Journal of Applied Polymer Science, **2012**, 124(4) 2999-3006.

[77] Osman, M.A., Ploetze, M. and Suter, U.W., *Surface treatment of clay minerals ? thermal stability, basal-plane spacing and surface coverage*. Journal of Materials Chemistry, **2003**, 13(9) 2359.

[78] Yoon, K., Sung, H., Hwang, Y.*, et al.*, *Modification of montmorillonite with oligomeric amine derivatives for polymer nanocomposite preparation*. Applied Clay Science, **2007**, 38(1-2) 1-8.

[79] Li, D., Liu, G., Wang, L.*, et al.*, *Preparation and thermo-oxidative degradation of poly(l-lactic acid)/poly(l-lactic acid)-grafted SiO2 nanocomposites*. Polymer Bulletin, **2011**, 67(8) 1529-1538.

[80] Leszczyńska, A., Njuguna, J., Pielichowski, K.*, et al.*, *Polymer/montmorillonite nanocomposites with improved thermal properties*. Thermochimica Acta, **2007**, 454(1) 1-22.

[81] Silvino, A.C., de Souza, K.S., Dahmouche, K.*, et al.*, *Polylactide/clay nanocomposites: A fresh look into the in situ polymerization process*. Journal of Applied Polymer Science, **2012**, 124(2) 1217-1224.

[82] Pluta, M., Galeski, A., Alexandre, M.*, et al.*, *Polylactide/montmorillonite nanocomposites and microcomposites prepared by melt blending: Structure and some physical properties*. Journal of Applied Polymer Science, **2002**, 86(6) 1497-1506.

[83] McLauchlin, A.R. and Thomas, N.L., *Preparation and thermal characterisation of poly(lactic acid) nanocomposites prepared from organoclays based on an amphoteric surfactant*. Polymer Degradation and Stability, **2009**, 94(5) 868-872.

[84] Kubies, D., Ščudla, J., Puffr, R.*, et al.*, *Structure and mechanical properties of poly(l-lactide)/layered silicate nanocomposites*. European Polymer Journal, **2006**, 42(4) 888-899.

[85] Galgali, G., Synthesis-structure-processing-property relationships in polymer nanocomposites. **2003**, PhD in National Chemical Laboratory.

[86] Kumar, A.P., Depan, D., Singh Tomer, N.*, et al.*, *Nanoscale particles for polymer degradation and stabilization—Trends and future perspectives*. Progress in Polymer Science, **2009**, 34(6) 479-515.

[87] Chow, W. and Lok, S., *Thermal properties of poly (lactic acid)/organo-montmorillonite nanocomposites*. Journal of thermal analysis and calorimetry, **2009**, 95(2) 627-632.

[88] Wu, X., Yuan, J., Yu, Y.*, et al.*, *Preparation and characterization of polylactide/montmorillonite nanocomposites*. Journal of Wuhan University of Technology--Materials Science Edition, **2009**, 24(4) 562-565.

[89] Paul, M.A., Alexandre, M., Degée, P.*, et al.*, *New nanocomposite materials based on plasticized poly (L-lactide) and organo-modified montmorillonites: thermal and morphological study*. Polymer, **2003**, 44(2) 443-450.

[90] Pavlidou, S. and Papaspyrides, C., *A review on polymer-layered silicate nanocomposites*. Progress in Polymer Science, **2008**, 33(12) 1119-1198.

[91] Silvestre, C., Duraccio, D. and Cimmino, S., *Food packaging based on polymer nanomaterials*. Progress in Polymer Science, **2011**, 36(12) 1766-1782.

[92] Goldstein, J., *Scanning electron microscopy and x-ray microanalysis*. **2003**, Kluwer Academic/Plenum Publishers, New York.

[93] Michler, G.H. and Godehardt, R., *Electron microscopy of polymers*. **2008**, Springer, Berlin.

[94] Gedde, U.W., *Polymer physics*. **1995**, Chapman & Hall, London; New York.

[95] Reimer, L., *Scanning electron microscopy : physics of image formation and microanalysis*. **1985**, Springer-Verlag, Berlin; New York.

[96] Peacock, A.J. and Calhoun, A.R., *Polymer chemistry properties and applications*. **2006**, Hanser Gardner Publications, Munich; Cincinnati, Ohio.

[97] Friedrich, K., Fakirov, S. and Zhang, Z., *Polymer composites : from nano- to macro-scale*. **2005**, Springer, New York.

[98] Sawyer, L.C., Grubb, D.T. and Meyers, G.F., *Polymer Microscopy*. **2008**, Springer New York, New York, NY.

[99] Koenig, J.L., *Spectroscopy of polymers*. **1992**, American Chemical Society, Washington, DC.

[100] Kumar, C.S.S.R., *Nanocomposites*. **2010**, Wiley-VCH, Weinheim.

[101] Subramani, K. and Ahmed, W., *Emerging nanotechnologies in dentistry processes, materials and applications*. **2012**, William Andrew, Oxford.

[102] Mittal, V., Kim, J.K. and Pal, K., *Recent Advances in Elastomeric Nanocomposites*. **2011**, Springer-Verlag Berlin Heidelberg, Berlin, Heidelberg.

[103] Nwabunma, D. and Kyu, T., *Polyolefin composites*. **2007**, John Wiley & Sons, Hoboken, N.J.

[104] Hatada, K. and Kitayama, T., *NMR spectroscopy of polymers*. **2004**, Springer, Berlin; London.

[105] Ibbett, R.N., *NMR spectroscopy of polymers*. **1993**, Blackie, London.

[106] Fawcett, A.H., *Polymer spectroscopy*. **1996**, Wiley, Chichester, England; New York.

[107] Flory, P.J., *Principles of polymer chemistry*. **1953**, Cornell University Press, Ithaca.

[108] Dealy, J.M. and Larson, R.G., *Structure and rheology of molten polymers : from structure to flow behavior and back again*. **2006**, Hanser Publishers ; Hanser Gardner Publications, Munich; Cincinnati.

[109] Mittal, V., *Characterization techniques for polymer nanocomposites*. **2012**, Wiley-VCH, Weinheim.

[110] Hatakeyama, T. and Quinn, F.X., *Thermal analysis : fundamentals and applications to polymer science*. **1999**, Wiley, Chichester.

[111] Lobo, H. and Bonilla, J.V., *Handbook of plastics analysis*. **2003**, Marcel Dekker, New York.

[112] Cheremisinoff, N.P., *Polymer characterization : laboratory techniques and analysis*. **1996**, Noyes Publications, Westwood, N.J.

[113] Crompton, T.R., *Polymer reference book*. **2006**, Rapra Technology Ltd., Shrewsbury, U.K.

[114] Tian, H. and Tagaya, H., *Preparation, characterization and mechanical properties of the polylactide/perlite and the polylactide/montmorillonite composites*. Journal of materials science, **2007**, 42(9) 3244-3250.

[115] Liu, X., Zou, Y., Li, W.*, et al.*, *Kinetics of thermo-oxidative and thermal degradation of poly(d,l-lactide) (PDLLA) at processing temperature*. Polymer Degradation and Stability, **2006**, 91(12) 3259-3265.

[116] Kister, G., Cassanas, G. and Vert, M., *Effects of morphology, conformation and configuration on the IR and Raman spectra of various poly (lactic acid) s*. Polymer, **1998**, 39(2) 267-273.

[117] Dadbin, S., Naimian, F. and Akhavan, A., *Poly (lactic acid)/layered silicate nanocomposite films: Morphology, mechanical properties, and effects of γ-radiation*. Journal of Applied Polymer Science, **2011**, 122(1) 142-149.

[118] Meaurio, E., Lopez-Rodriguez, N. and Sarasua, J., *Infrared spectrum of poly (L-lactide): Application to crystallinity studies*. Macromolecules, **2006**, 39(26) 9291-9301.

[119] Matusik, J., Stodolak, E. and Bahranowski, K., *Synthesis of polylactide/clay composites using structurally different kaolinites and kaolinite nanotubes*. Applied Clay Science, **2011**, 51(1-2) 102-109.

[120] Gardette, M., Thérias, S., Gardette, J.-L.*, et al.*, *Photooxidation of polylactide/calcium sulphate composites*. Polymer Degradation and Stability, **2011**, 96(4) 616-623.

[121] Zaidi, L., Kaci, M., Bruzaud, S.*, et al.*, *Effect of natural weather on the structure and properties of polylactide/Cloisite 30B nanocomposites*. Polymer Degradation and Stability, **2010**, 95(9) 1751-1758.

[122] Bocchini, S., Fukushima, K., Blasio, A.D.*, et al.*, *Polylactic Acid and Polylactic Acid-Based Nanocomposite Photooxidation*. Biomacromolecules, **2010**, 11(11) 2919-1926.

[123] Wu, T.-M. and Wu, C.-Y., *Biodegradable poly(lactic acid)/chitosan-modified montmorillonite nanocomposites: Preparation and characterization*. Polymer Degradation and Stability, **2006**, 91(9) 2198-2204.

[124] Solarski, S., Mahjoubi, F., Ferreira, M.*, et al.*, *(Plasticized) Polylactide/clay nanocomposite textile: thermal, mechanical, shrinkage and fire properties*. Journal of materials science, **2007**, 42(13) 5105-5117.

[125] Sinha Ray, S. and Okamoto, M., *Polymer/layered silicate nanocomposites: a review from preparation to processing*. Progress in Polymer Science, **2003**, 28(11) 1539-1641.

[126] Fukushima, K., Abbate, C., Tabuani, D.*, et al.*, *Biodegradation of poly(lactic acid) and its nanocomposites*. Polymer Degradation and Stability, **2009**, 94(10) 1646-1655.

[127] Leszczyńska, A., Njuguna, J., Pielichowski, K.*, et al.*, *Polymer/montmorillonite nanocomposites with improved thermal properties*. Thermochimica Acta, **2007**, 453(2) 75-96.

[128] Carrasco, F., Pagès, P., Gámez-Pérez, J., *et al.*, *Processing of poly(lactic acid): Characterization of chemical structure, thermal stability and mechanical properties*. Polymer Degradation and Stability, **2010**, 95(2) 116-125.

[129] Solarski, S., Ferreira, M. and Devaux, E., *Ageing of polylactide and polylactide nanocomposite filaments*. Polymer Degradation and Stability, **2008**, 93(3) 707-713.

[130] Lewitus, D., McCarthy, S., Ophir, A., *et al.*, *The effect of nanoclays on the properties of PLLA-modified polymers part 1: mechanical and thermal properties*. Journal of Polymers and the Environment, **2006**, 14(2) 171-177.

[131] Tsuji, H., Sugiyama, H. and Sato, Y., *Photodegradation of Poly (lactic acid) Stereocomplex by UV-Irradiation*. Journal of Polymers and the Environment, **2012**, 1-7.

[132] Janorkar, A.V., Metters, A.T. and Hirt, D.E., *Degradation of poly (L-lactide) films under ultraviolet-induced photografting and sterilization conditions*. Journal of Applied Polymer Science, **2007**, 106(2) 1042-1047.